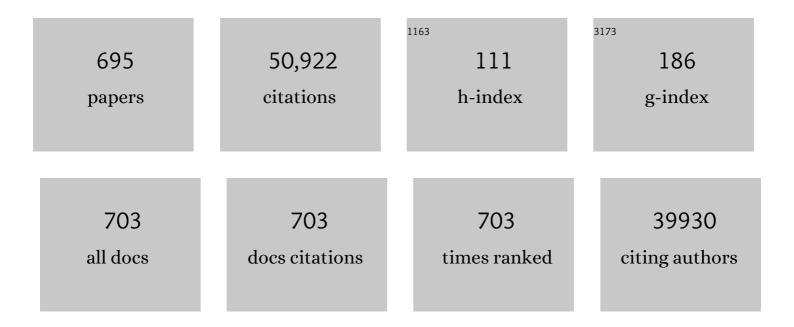
List of Publications by Year in descending order

Source: https://exaly.com/author-pdf/5694476/publications.pdf Version: 2024-02-01



ILE-SHAN OUL

#	Article	IF	CITATIONS
1	Flexible and conductive MXene films and nanocomposites with high capacitance. Proceedings of the National Academy of Sciences of the United States of America, 2014, 111, 16676-16681.	3.3	1,713
2	Ultralight and Highly Compressible Graphene Aerogels. Advanced Materials, 2013, 25, 2219-2223.	11.1	1,249
3	Preparation and Characterization of Multiwalled Carbon Nanotube-Supported Platinum for Cathode Catalysts of Direct Methanol Fuel Cells. Journal of Physical Chemistry B, 2003, 107, 6292-6299.	1.2	1,079
4	Enhancing lithium–sulphur battery performance by strongly binding the discharge products on amino-functionalized reduced graphene oxide. Nature Communications, 2014, 5, 5002.	5.8	892
5	Metal–Organicâ€Frameworkâ€Đerived Hybrid Carbon Nanocages as a Bifunctional Electrocatalyst for Oxygen Reduction and Evolution. Advanced Materials, 2017, 29, 1700874.	11.1	678
6	Electroactive edge site-enriched nickel–cobalt sulfide into graphene frameworks for high-performance asymmetric supercapacitors. Energy and Environmental Science, 2016, 9, 1299-1307.	15.6	623
7	Sustainable Synthesis and Assembly of Biomassâ€Derived B/N Coâ€Doped Carbon Nanosheets with Ultrahigh Aspect Ratio for Highâ€Performance Supercapacitors. Advanced Functional Materials, 2016, 26, 111-119.	7.8	607
8	Stabilizing the MXenes by Carbon Nanoplating for Developing Hierarchical Nanohybrids with Efficient Lithium Storage and Hydrogen Evolution Capability. Advanced Materials, 2017, 29, 1607017.	11.1	583
9	High performance hybrid solar cells sensitized by organolead halide perovskites. Energy and Environmental Science, 2013, 6, 1480.	15.6	582
10	Design and fabrication of carbon dots for energy conversion and storage. Chemical Society Reviews, 2019, 48, 2315-2337.	18.7	552
11	Boosting electrocatalytic oxygen evolution by synergistically coupling layered double hydroxide with MXene. Nano Energy, 2018, 44, 181-190.	8.2	458
12	Low-cost dye-sensitized solar cell based on nine kinds of carbon counter electrodes. Energy and Environmental Science, 2011, 4, 2308.	15.6	434
13	Aggregation-Resistant 3D MXene-Based Architecture as Efficient Bifunctional Electrocatalyst for Overall Water Splitting. ACS Nano, 2018, 12, 8017-8028.	7.3	425
14	Carbon nanotubes as support for cathode catalyst of a direct methanol fuel cell. Carbon, 2002, 40, 791-794.	5.4	402
15	Carbon foam: Preparation and application. Carbon, 2015, 87, 128-152.	5.4	347
16	High energy-power Zn-ion hybrid supercapacitors enabled by layered B/N co-doped carbon cathode. Nano Energy, 2019, 66, 104132.	8.2	344
17	Activated carbon nanofiber webs made by electrospinning for capacitive deionization. Electrochimica Acta, 2012, 69, 65-70.	2.6	334
18	Efficient preparation of biomass-based mesoporous carbons for supercapacitors with both high energy density and high power density. Journal of Power Sources, 2013, 240, 109-113.	4.0	329

#	Article	IF	CITATIONS
19	A Layeredâ€Nanospaceâ€Confinement Strategy for the Synthesis of Twoâ€Dimensional Porous Carbon Nanosheets for Highâ€Rate Performance Supercapacitors. Advanced Energy Materials, 2015, 5, 1401761.	10.2	308
20	Ultrafine MoO ₂ â€Carbon Microstructures Enable Ultralongâ€Life Powerâ€Type Sodium Ion Storage by Enhanced Pseudocapacitance. Advanced Energy Materials, 2017, 7, 1602880.	10.2	306
21	Synthesis of Fe3O4@ZIF-8 magnetic core–shell microspheres and their potential application in a capillary microreactor. Chemical Engineering Journal, 2013, 228, 398-404.	6.6	301
22	Superhierarchical Cobaltâ€Embedded Nitrogenâ€Doped Porous Carbon Nanosheets as Twoâ€inâ€One Hosts for Highâ€Performance Lithium–Sulfur Batteries. Advanced Materials, 2018, 30, e1706895.	11.1	300
23	A superhydrophilic "nanoglue―for stabilizing metal hydroxides onto carbon materials for high-energy and ultralong-life asymmetric supercapacitors. Energy and Environmental Science, 2017, 10, 1958-1965.	15.6	294
24	A Flexible TiO ₂ (B)â€Based Battery Electrode with Superior Power Rate and Ultralong Cycle Life. Advanced Materials, 2013, 25, 3462-3467.	11.1	286
25	A hierarchically porous and hydrophilic 3D nickel–iron/MXene electrode for accelerating oxygen and hydrogen evolution at high current densities. Nano Energy, 2019, 63, 103880.	8.2	275
26	Strategies to suppress hydrogen evolution for highly selective electrocatalytic nitrogen reduction: challenges and perspectives. Energy and Environmental Science, 2021, 14, 1176-1193.	15.6	275
27	Enhanced sodium storage capability enabled by super wide-interlayer-spacing MoS2 integrated on carbon fibers. Nano Energy, 2017, 41, 66-74.	8.2	273
28	Iron-tuned super nickel phosphide microstructures with high activity for electrochemical overall water splitting. Nano Energy, 2017, 34, 472-480.	8.2	258
29	Synthesis of mesoporous carbons for supercapacitors from coal tar pitch by coupling microwave-assisted KOH activation with a MgO template. Carbon, 2012, 50, 4911-4921.	5.4	256
30	Electrochemical ammonia synthesis: Mechanistic understanding and catalyst design. CheM, 2021, 7, 1708-1754.	5.8	253
31	3D Architecture Materials Made of NiCoAlâ€LDH Nanoplates Coupled with NiCoâ€Carbonate Hydroxide Nanowires Grown on Flexible Graphite Paper for Asymmetric Supercapacitors. Advanced Energy Materials, 2014, 4, 1400761.	10.2	251
32	The role of microwave absorption on formation of graphene from graphite oxide. Carbon, 2012, 50, 3267-3273.	5.4	250
33	Energy-saving hydrogen production by chlorine-free hybrid seawater splitting coupling hydrazine degradation. Nature Communications, 2021, 12, 4182.	5.8	233
34	Strategies and insights towards the intrinsic capacitive properties of MnO2 for supercapacitors: Challenges and perspectives. Nano Energy, 2019, 57, 459-472.	8.2	232
35	3D Porous Nâ€Đoped Graphene Frameworks Made of Interconnected Nanocages for Ultrahighâ€Rate and Long‣ife Li–O ₂ Batteries. Advanced Functional Materials, 2015, 25, 6913-6920.	7.8	231
36	Ultrafast Selfâ€Assembly of Graphene Oxideâ€Induced Monolithic NiCo–Carbonate Hydroxide Nanowire Architectures with a Superior Volumetric Capacitance for Supercapacitors. Advanced Functional Materials, 2015, 25, 2109-2116.	7.8	230

#	Article	IF	CITATIONS
37	Engineering hollow polyhedrons structured from carbon-coated CoSe ₂ nanospheres bridged by CNTs with boosted sodium storage performance. Journal of Materials Chemistry A, 2017, 5, 13591-13600.	5.2	225
38	Activated TiO2 with tuned vacancy for efficient electrochemical nitrogen reduction. Applied Catalysis B: Environmental, 2019, 257, 117896.	10.8	220
39	Facile synthesis of sandwich-like polyaniline/boron-doped graphene nano hybrid for supercapacitors. Carbon, 2015, 81, 552-563.	5.4	218
40	Nitrogen-doped activated carbon derived from prawn shells for high-performance supercapacitors. Electrochimica Acta, 2016, 190, 1134-1141.	2.6	217
41	Ultrasensitive Ironâ€Triggered Nanosized Fe–CoOOH Integrated with Graphene for Highly Efficient Oxygen Evolution. Advanced Energy Materials, 2017, 7, 1602148.	10.2	216
42	Surface modification of biomass-derived hard carbon by grafting porous carbon nanosheets for high-performance supercapacitors. Journal of Materials Chemistry A, 2018, 6, 15954-15960.	5.2	216
43	Hierarchical activated carbon nanofiber webs with tuned structure fabricated by electrospinning for capacitive deionization. Journal of Materials Chemistry, 2012, 22, 21819.	6.7	215
44	Surfaceâ€Confined Fabrication of Ultrathin Nickel Cobaltâ€Layered Double Hydroxide Nanosheets for Highâ€Performance Supercapacitors. Advanced Functional Materials, 2018, 28, 1803272.	7.8	215
45	Compressible Carbon Nanotube–Graphene Hybrid Aerogels with Superhydrophobicity and Superoleophilicity for Oil Sorption. Environmental Science and Technology Letters, 2014, 1, 214-220.	3.9	212
46	ZnO template strategy for the synthesis of 3D interconnected graphene nanocapsules from coal tar pitch as supercapacitor electrode materials. Journal of Power Sources, 2017, 340, 183-191.	4.0	212
47	Preparation of functionalized water-soluble photoluminescent carbon quantum dots from petroleum coke. Carbon, 2014, 78, 480-489.	5.4	210
48	A Topâ€Down Strategy toward 3D Carbon Nanosheet Frameworks Decorated with Hollow Nanostructures for Superior Lithium Storage. Advanced Functional Materials, 2016, 26, 7590-7598.	7.8	201
49	New Membrane Architecture with High Performance: ZIF-8 Membrane Supported on Vertically Aligned ZnO Nanorods for Gas Permeation and Separation. Chemistry of Materials, 2014, 26, 1975-1981.	3.2	199
50	Highly mesoporous activated carbon electrode for capacitive deionization. Separation and Purification Technology, 2013, 103, 216-221.	3.9	198
51	Engineering Multifunctional Collaborative Catalytic Interface Enabling Efficient Hydrogen Evolution in All pH Range and Seawater. Advanced Energy Materials, 2019, 9, 1901333.	10.2	196
52	Facile fabrication of MWCNT-doped NiCoAl-layered double hydroxide nanosheets with enhanced electrochemical performances. Journal of Materials Chemistry A, 2013, 1, 1963-1968.	5.2	193
53	Highly efficient synthesis of graphene/MnO2 hybrids and their application for ultrafast oxidative decomposition of methylene blue. Carbon, 2014, 66, 485-492.	5.4	189
54	Highly Stretchable and Ultrasensitive Strain Sensor Based on Reduced Graphene Oxide Microtubes–Elastomer Composite. ACS Applied Materials & Interfaces, 2015, 7, 27432-27439.	4.0	189

#	Article	IF	CITATIONS
55	Electrochemical CO2 reduction to C2+ species: Heterogeneous electrocatalysts, reaction pathways, and optimization strategies. Materials Today Energy, 2018, 10, 280-301.	2.5	188
56	Recent advances in innovative strategies for the CO ₂ electroreduction reaction. Energy and Environmental Science, 2021, 14, 765-780.	15.6	188
57	Chemically Tailoring Coal to Fluorescent Carbon Dots with Tuned Size and Their Capacity for Cu(II) Detection. Small, 2014, 10, 4926-4933.	5.2	186
58	Carbon-supported Ni nanoparticles for efficient CO ₂ electroreduction. Chemical Science, 2018, 9, 8775-8780.	3.7	179
59	Perspectives on solution processing of two-dimensional MXenes. Materials Today, 2021, 48, 214-240.	8.3	178
60	Nanohybrids from NiCoAl-LDH coupled with carbon for pseudocapacitors: understanding the role of nano-structured carbon. Nanoscale, 2014, 6, 3097-3104.	2.8	176
61	NiCo-layered double hydroxides vertically assembled on carbon fiber papers as binder-free high-active electrocatalysts for water oxidation. Carbon, 2016, 110, 1-7.	5.4	175
62	Ag/SiO2: a novel catalyst with high activity and selectivity for hydrogenation of chloronitrobenzenes. Chemical Communications, 2005, , 5298.	2.2	174
63	Restructuring of Cu ₂ O to Cu ₂ O@Cu-Metal–Organic Frameworks for Selective Electrochemical Reduction of CO ₂ . ACS Applied Materials & Interfaces, 2019, 11, 9904-9910.	4.0	174
64	Hydrothermal synthesis and activation of graphene-incorporated nitrogen-rich carbon composite for high-performance supercapacitors. Carbon, 2014, 70, 130-141.	5.4	171
65	P/N co-doped microporous carbons from H3PO4-doped polyaniline by in situ activation for supercapacitors. Carbon, 2013, 59, 537-546.	5.4	169
66	Direct synthesis of 3D hollow porous graphene balls from coal tar pitch for high performance supercapacitors. Journal of Materials Chemistry A, 2014, 2, 19633-19640.	5.2	169
67	Formation of two-dimensional transition metal oxide nanosheets with nanoparticles as intermediates. Nature Materials, 2019, 18, 970-976.	13.3	169
68	Rapid and energy-efficient microwave pyrolysis for high-yield production of highly-active bifunctional electrocatalysts for water splitting. Energy and Environmental Science, 2020, 13, 545-553.	15.6	169
69	A layered-template-nanospace-confinement strategy for production of corrugated graphene nanosheets from petroleum pitch for supercapacitors. Chemical Engineering Journal, 2016, 297, 121-127.	6.6	168
70	Surface-treated carbon electrodes with modified potential of zero charge for capacitive deionization. Water Research, 2016, 93, 30-37.	5.3	168
71	Toward commercial-level mass-loading electrodes for supercapacitors: opportunities, challenges and perspectives. Energy and Environmental Science, 2021, 14, 576-601.	15.6	166
72	Mass and Charge Transfer Coenhanced Oxygen Evolution Behaviors in CoFe‣ayered Double Hydroxide Assembled on Graphene. Advanced Materials Interfaces, 2016, 3, 1500782.	1.9	165

#	Article	IF	CITATIONS
73	MXene-Based Electrode with Enhanced Pseudocapacitance and Volumetric Capacity for Power-Type and Ultra-Long Life Lithium Storage. ACS Nano, 2018, 12, 3928-3937.	7.3	163
74	Sustainable synthesis of phosphorus- and nitrogen-co-doped porous carbons with tunable surface properties for supercapacitors. Journal of Power Sources, 2013, 239, 81-88.	4.0	162
75	Synthesis of hierarchical porous carbons for supercapacitors from coal tar pitch with nano-Fe2O3 as template and activation agent coupled with KOH activation. Journal of Materials Chemistry A, 2013, 1, 9440.	5.2	162
76	Nitrogen-doped carbon dots decorated on graphene: a novel all-carbon hybrid electrocatalyst for enhanced oxygen reduction reaction. Chemical Communications, 2015, 51, 3419-3422.	2.2	157
77	Scrutinizing Defects and Defect Density of Seleniumâ€Doped Graphene for Highâ€Efficiency Triiodide Reduction in Dyeâ€Sensitized Solar Cells. Angewandte Chemie - International Edition, 2018, 57, 4682-4686.	7.2	155
78	Ultrahigh Rate and Longâ€Life Sodiumâ€Ion Batteries Enabled by Engineered Surface and Nearâ€Surface Reactions. Advanced Materials, 2018, 30, 1702486.	11.1	153
79	Freestanding Flexible Li ₂ S Paper Electrode with High Mass and Capacity Loading for Highâ€Energy Li–S Batteries. Advanced Energy Materials, 2017, 7, 1700018.	10.2	152
80	Boric acid-mediated B,N-codoped chitosan-derived porous carbons with a high surface area and greatly improved supercapacitor performance. Nanoscale, 2015, 7, 5120-5125.	2.8	151
81	Porous carbon nanosheets from coal tar for high-performance supercapacitors. Journal of Power Sources, 2017, 357, 41-46.	4.0	150
82	Oxygen vacancy enables electrochemical N2 fixation over WO3 with tailored structure. Nano Energy, 2019, 62, 869-875.	8.2	150
83	Multilevel Hollow MXene Tailored Lowâ€Pt Catalyst for Efficient Hydrogen Evolution in Fullâ€pH Range and Seawater. Advanced Functional Materials, 2020, 30, 1910028.	7.8	150
84	Cobalt-embedded nitrogen-doped hollow carbon nanorods for synergistically immobilizing the discharge products in lithium–sulfur battery. Energy Storage Materials, 2016, 5, 223-229.	9.5	149
85	Nitrogenâ€Ðoped Graphene Nanoribbons with Surface Enriched Active Sites and Enhanced Performance for Dyeâ€Sensitized Solar Cells. Advanced Energy Materials, 2015, 5, 1500180.	10.2	147
86	Homogeneous and controllable Pt particles deposited on multi-wall carbon nanotubes as cathode catalyst for direct methanol fuel cells. Carbon, 2004, 42, 436-439.	5.4	142
87	Photocatalytic Fixation of Nitrogen to Ammonia by Single Ru Atom Decorated TiO ₂ Nanosheets. ACS Sustainable Chemistry and Engineering, 2019, 7, 6813-6820.	3.2	142
88	Polymer/Graphene Hybrid Aerogel with High Compressibility, Conductivity, and "Sticky― Superhydrophobicity. ACS Applied Materials & Interfaces, 2014, 6, 3242-3249.	4.0	140
89	A simple and scalable method for preparing low-defect ZIF-8 tubular membranes. Journal of Materials Chemistry A, 2013, 1, 10635.	5.2	139
90	Thinâ€Sheet Carbon Nanomesh with an Excellent Electrocapacitive Performance. Advanced Functional Materials, 2015, 25, 5420-5427.	7.8	139

#	Article	IF	CITATIONS
91	Graphene Sheets from Graphitized Anthracite Coal: Preparation, Decoration, and Application. Energy & Fuels, 2012, 26, 5186-5192.	2.5	136
92	Preparation of coal-based microfiltration carbon membrane and application in oily wastewater treatment. Separation and Purification Technology, 2006, 51, 80-84.	3.9	133
93	Asymmetric capacitive deionization utilizing nitric acid treated activated carbon fiber as the cathode. Electrochimica Acta, 2015, 176, 426-433.	2.6	130
94	N/P-Codoped Thermally Reduced Graphene for High-Performance Supercapacitor Applications. Journal of Physical Chemistry C, 2013, 117, 14912-14919.	1.5	128
95	Carbon-Stabilized Interlayer-Expanded Few-Layer MoSe ₂ Nanosheets for Sodium Ion Batteries with Enhanced Rate Capability and Cycling Performance. ACS Applied Materials & Interfaces, 2016, 8, 32324-32332.	4.0	128
96	Mesoporous microspheres composed of carbon-coated TiO2 nanocrystals with exposed {001} facets for improved visible light photocatalytic activity. Applied Catalysis B: Environmental, 2014, 147, 958-964.	10.8	127
97	Zinc-blende ZnO and its role in nucleating wurtzite tetrapods and twinned nanowires. Applied Physics Letters, 2007, 90, 153510.	1.5	126
98	Effect of activation time on the properties of activated carbons prepared by microwave-assisted activation for electric double layer capacitors. Carbon, 2010, 48, 1662-1669.	5.4	126
99	Aerobic oxidation of alcohols over carbon nanotube-supported Ru catalysts assembled at the interfaces of emulsion droplets. Applied Catalysis A: General, 2010, 382, 131-137.	2.2	124
100	Highly Stable Hybrid Capacitive Deionization with a MnO ₂ Anode and a Positively Charged Cathode. Environmental Science and Technology Letters, 2018, 5, 98-102.	3.9	124
101	Solvothermal conversion of coal into nitrogen-doped carbon dots with singlet oxygen generation and high quantum yield. Chemical Engineering Journal, 2017, 320, 570-575.	6.6	123
102	Cascade charge transfer enabled by incorporating edge-enriched graphene nanoribbons for mesostructured perovskite solar cells with enhanced performance. Nano Energy, 2018, 52, 123-133.	8.2	123
103	A green strategy for the synthesis of graphene supported Mn 3 O 4 nanocomposites from graphitized coal and their supercapacitor application. Carbon, 2014, 80, 640-650.	5.4	121
104	Rice husk-based hierarchical porous carbon for high performance supercapacitors: The structure-performance relationship. Carbon, 2020, 161, 432-444.	5.4	121
105	Starch Derived Porous Carbon Nanosheets for High-Performance Photovoltaic Capacitive Deionization. Environmental Science & amp; Technology, 2017, 51, 9244-9251.	4.6	120
106	In situ fabrication of a perfect Pd/ZnO@ZIF-8 core–shell microsphere as an efficient catalyst by a ZnO support-induced ZIF-8 growth strategy. Nanoscale, 2015, 7, 7615-7623.	2.8	118
107	Selective catalytic reduction of nitrogen oxides by ammonia over Co3O4 nanocrystals with different shapes. Applied Catalysis B: Environmental, 2013, 129, 491-500.	10.8	117
108	Bridging of Ultrathin NiCo ₂ O ₄ Nanosheets and Graphene with Polyaniline: A Theoretical and Experimental Study. Chemistry of Materials, 2016, 28, 5855-5863.	3.2	116

#	Article	IF	CITATIONS
109	A Polymetallic Metalâ€Organic Frameworkâ€Derived Strategy toward Synergistically Multidoped Metal Oxide Electrodes with Ultralong Cycle Life and High Volumetric Capacity. Advanced Functional Materials, 2017, 27, 1605332.	7.8	116
110	GO-guided direct growth of highly oriented metal–organic framework nanosheet membranes for H ₂ /CO ₂ separation. Chemical Science, 2018, 9, 4132-4141.	3.7	116
111	Membrane-Free Hybrid Capacitive Deionization System Based on Redox Reaction for High-Efficiency NaCl Removal. Environmental Science & Technology, 2019, 53, 6292-6301.	4.6	116
112	Electrospun Composites Made of Reduced Graphene Oxide and Activated Carbon Nanofibers for Capacitive Deionization. Electrochimica Acta, 2014, 137, 388-394.	2.6	115
113	A simple and efficient protocol for a palladium-catalyzed ligand-free Suzuki reaction at room temperature in aqueous DMF. Green Chemistry, 2011, 13, 1260.	4.6	114
114	Interlayer expanded MoS 2 enabled by edge effect of graphene nanoribbons for high performance lithium and sodium ion batteries. Carbon, 2016, 109, 461-471.	5.4	114
115	Highly stable two-dimensional bismuth metal-organic frameworks for efficient electrochemical reduction of CO2. Applied Catalysis B: Environmental, 2020, 277, 119241.	10.8	109
116	Recent research advances of self-discharge in supercapacitors: Mechanisms and suppressing strategies. Journal of Energy Chemistry, 2021, 58, 94-109.	7.1	109
117	A rapid synthesis route for Sn-Beta zeolites by steam-assisted conversion and their catalytic performance in Baeyer–Villiger oxidation. Chemical Engineering Journal, 2013, 218, 425-432.	6.6	107
118	Hydrothermal Synthesis of Phosphate-Functionalized Carbon Nanotube-Containing Carbon Composites for Supercapacitors with Highly Stable Performance. ACS Applied Materials & Interfaces, 2013, 5, 2104-2110.	4.0	107
119	Boron-doped graphene as a high-efficiency counter electrode for dye-sensitized solar cells. Chemical Communications, 2014, 50, 3328.	2.2	107
120	Interconnected sheet-like porous carbons from coal tar by a confined soft-template strategy for supercapacitors. Chemical Engineering Journal, 2018, 350, 49-56.	6.6	107
121	Luminescent Properties of Metal–Organic Framework MOF-5: Relativistic Time-Dependent Density Functional Theory Investigations. Inorganic Chemistry, 2012, 51, 12389-12394.	1.9	106
122	Sulfur-infiltrated graphene-backboned mesoporous carbon nanosheets with a conductive polymer coating for long-life lithium–sulfur batteries. Nanoscale, 2015, 7, 7569-7573.	2.8	106
123	Construction of 3D nanostructure hierarchical porous graphitic carbons by charge-induced self-assembly and nanocrystal-assisted catalytic graphitization for supercapacitors. Chemical Communications, 2016, 52, 6673-6676.	2.2	106
124	Hierarchical porous carbon sheets derived from biomass containing an activation agent and in-built template for lithium ion batteries. Carbon, 2018, 139, 1085-1092.	5.4	106
125	Nitrogen-doped hierarchically porous carbon nanosheets derived from polymer/graphene oxide hydrogels for high-performance supercapacitors. Journal of Colloid and Interface Science, 2020, 560, 69-76.	5.0	106
126	Ultrasound-assisted preparation of electrospun carbon fiber/graphene electrodes for capacitive deionization: Importance and unique role of electrical conductivity. Carbon, 2016, 103, 311-317.	5.4	105

#	Article	IF	CITATIONS
127	Flexible Paper-like Free-Standing Electrodes by Anchoring Ultrafine SnS ₂ Nanocrystals on Graphene Nanoribbons for High-Performance Sodium Ion Batteries. ACS Applied Materials & Interfaces, 2017, 9, 15484-15491.	4.0	102
128	Progress and prospects of hydrogen production: Opportunities and challenges. Journal of Electronic Science and Technology, 2021, 19, 100080.	2.0	102
129	Ultrafast Fabrication of Covalently Crossâ€ŀinked Multifunctional Graphene Oxide Monoliths. Advanced Functional Materials, 2014, 24, 4915-4921.	7.8	101
130	Cellular carbon-wrapped FeSe ₂ nanocavities with ultrathin walls and multiple rooms for ion diffusion-confined ultrafast sodium storage. Journal of Materials Chemistry A, 2019, 7, 4469-4479.	5.2	101
131	Design and Fabrication of Hierarchical NiCoP–MOF Heterostructure with Enhanced Pseudocapacitive Properties. Small, 2021, 17, e2100353.	5.2	101
132	A simple and efficient approach for the palladium-catalyzed ligand-free Suzuki reaction in water. Green Chemistry, 2012, 14, 2999.	4.6	100
133	Hydrothermal synthesis and electrochemical performance of Co3O4/reduced graphene oxide nanosheet composites for supercapacitors. Electrochimica Acta, 2013, 112, 120-126.	2.6	100
134	Graphene-mediated highly-dispersed MoS2 nanosheets with enhanced triiodide reduction activity for dye-sensitized solar cells. Carbon, 2016, 100, 474-483.	5.4	100
135	Synthesis of a carbon nanofiber/carbon foam composite from coal liquefaction residue for the separation of oil and water. Carbon, 2013, 59, 530-536.	5.4	99
136	Dually Fixed SnO ₂ Nanoparticles on Graphene Nanosheets by Polyaniline Coating for Superior Lithium Storage. ACS Applied Materials & Interfaces, 2015, 7, 2444-2451.	4.0	99
137	Preparation of carbon nanosheets from petroleum asphalt via recyclable molten-salt method for superior lithium and sodium storage. Carbon, 2017, 122, 344-351.	5.4	99
138	BCN nanosheets templated by g-C ₃ N ₄ for high performance capacitive deionization. Journal of Materials Chemistry A, 2018, 6, 14644-14650.	5.2	99
139	Efficient CO2 electroreduction over pyridinic-N active sites highly exposed on wrinkled porous carbon nanosheets. Chemical Engineering Journal, 2018, 351, 613-621.	6.6	99
140	Organic electron-rich N-heterocyclic compound as a chemical bridge: building a Brönsted acidic ionic liquid confined in MIL-101 nanocages. Journal of Materials Chemistry A, 2013, 1, 6530.	5.2	98
141	Coal-based carbon anodes for high-performance potassium-ion batteries. Carbon, 2019, 147, 574-581.	5.4	98
142	Nitrogen-doped soft carbon frameworks built of well-interconnected nanocapsules enabling a superior potassium-ion batteries anode. Chemical Engineering Journal, 2020, 382, 121759.	6.6	98
143	Low temperature plasma synthesis of mesoporous Fe3O4 nanorods grafted on reduced graphene oxide for high performance lithium storage. Nanoscale, 2014, 6, 2286.	2.8	97
144	Pitch-derived N-doped porous carbon nanosheets with expanded interlayer distance as high-performance sodium-ion battery anodes. Fuel Processing Technology, 2018, 177, 328-335.	3.7	97

#	Article	IF	CITATIONS
145	3D nickel-cobalt phosphide heterostructure for high-performance solid-state hybrid supercapacitors. Journal of Power Sources, 2020, 467, 228324.	4.0	97
146	High-yield production of few-layer boron nanosheets for efficient electrocatalytic N ₂ reduction. Chemical Communications, 2019, 55, 4246-4249.	2.2	96
147	Energy‣aving Hydrogen Production by Seawater Electrolysis Coupling Sulfion Degradation. Advanced Materials, 2022, 34, e2109321.	11.1	95
148	A novel form of carbon micro-balls from coal. Carbon, 2003, 41, 767-772.	5.4	94
149	Aerobic oxidation of alcohols over Au/TiO2: An insight on the promotion effect of water on the catalytic activity of Au/TiO2. Catalysis Communications, 2008, 9, 2278-2281.	1.6	92
150	Ultrasound-assisted preparation of electrospun carbon nanofiber/graphene composite electrode for supercapacitors. Journal of Power Sources, 2013, 243, 350-353.	4.0	92
151	Hydrodeoxygenation of vanillin over carbon nanotube-supported Ru catalysts assembled at the interfaces of emulsion droplets. Catalysis Communications, 2014, 47, 28-31.	1.6	92
152	High-energy quasi-solid-state supercapacitors enabled by carbon nanofoam from biowaste and high-voltage inorganic gel electrolyte. Carbon, 2019, 149, 273-280.	5.4	91
153	N, P co-doped hierarchical porous carbon from rapeseed cake with enhanced supercapacitance. Renewable Energy, 2021, 170, 188-196.	4.3	91
154	Decoupling and correlating the ion transport by engineering 2D carbon nanosheets for enhanced charge storage. Nano Energy, 2019, 64, 103921.	8.2	90
155	Micro-sized porous carbon spheres with ultra-high rate capability for lithium storage. Nanoscale, 2015, 7, 1791-1795.	2.8	88
156	Operando Revealing Dynamic Reconstruction of NiCo Carbonate Hydroxide for High-Rate Energy Storage. Joule, 2020, 4, 673-687.	11.7	88
157	Understanding of Sodium Storage Mechanism in Hard Carbons: Ongoing Development under Debate. Advanced Energy Materials, 2022, 12, .	10.2	88
158	Chemically grafting graphene oxide to B,N co-doped graphene via ionic liquid and their superior performance for triiodide reduction. Nano Energy, 2016, 25, 184-192.	8.2	87
159	Rational design of high-performance sodium-ion battery anode by molecular engineering of coal tar pitch. Chemical Engineering Journal, 2018, 342, 52-60.	6.6	87
160	Nitrogen-doped porous carbon from coal for high efficiency CO2 electrocatalytic reduction. Carbon, 2019, 151, 46-52.	5.4	87
161	Graphene-based materials for electrochemical CO2 reduction. Journal of CO2 Utilization, 2019, 30, 168-182.	3.3	87
162	Accelerating polysulfide redox conversion on bifunctional electrocatalytic electrode for stable Li-S batteries. Energy Storage Materials, 2019, 20, 98-107.	9.5	87

#	Article	IF	CITATIONS
163	Preparation and characterization of porous carbons from PAN-based preoxidized cloth by KOH activation. Carbon, 2004, 42, 205-210.	5.4	86
164	Lightweight carbon foam from coal liquefaction residue with broad-band microwave absorbing capability. Carbon, 2016, 105, 224-226.	5.4	86
165	Synthesis of ultrathin hollow carbon shell from petroleum asphalt for high-performance anode material in lithium-ion batteries. Chemical Engineering Journal, 2016, 286, 632-639.	6.6	86
166	Ultrafine MoO3 anchored in coal-based carbon nanofibers as anode for advanced lithium-ion batteries. Carbon, 2020, 156, 445-452.	5.4	84
167	Oxygen-promoted PdCl ₂ -catalyzed ligand-free Suzuki reaction in aqueous media. Organic and Biomolecular Chemistry, 2011, 9, 1054-1060.	1.5	83
168	Highâ€Stackingâ€Density, Superiorâ€Roughness LDH Bridged with Vertically Aligned Graphene for Highâ€Performance Asymmetric Supercapacitors. Small, 2017, 13, 1701288.	5.2	83
169	Engineering cross-linking by coal-based graphene quantum dots toward tough, flexible, and hydrophobic electrospun carbon nanofiber fabrics. Carbon, 2018, 129, 54-62.	5.4	83
170	Fabrication and characterization of magnetic Fe3O4–CNT composites. Journal of Physics and Chemistry of Solids, 2010, 71, 673-676.	1.9	82
171	Strongly Coupled Architectures of Cobalt Phosphide Nanoparticles Assembled on Graphene as Bifunctional Electrocatalysts for Water Splitting. ChemElectroChem, 2016, 3, 719-725.	1.7	82
172	Highly Efficient Lowâ€Temperature Plasmaâ€Assisted Modification of TiO ₂ Nanosheets with Exposed {001} Facets for Enhanced Visibleâ€Light Photocatalytic Activity. Chemistry - A European Journal, 2014, 20, 14763-14770.	1.7	81
173	Activation of transition metal oxides by in-situ electro-regulated structure-reconstruction for ultra-efficient oxygen evolution. Nano Energy, 2019, 58, 778-785.	8.2	81
174	A Universal Converse Voltage Process for Triggering Transition Metal Hybrids In Situ Phase Restruction toward Ultrahighâ€Rate Supercapacitors. Advanced Materials, 2019, 31, e1901241.	11.1	81
175	CVD synthesis of coal-gas-derived carbon nanotubes and nanocapsules containing magnetic iron carbide and oxide. Carbon, 2006, 44, 2565-2568.	5.4	80
176	Ultrastable and high-capacity carbon nanofiber anodes derived from pitch/polyacrylonitrile for flexible sodium-ion batteries. Carbon, 2018, 135, 187-194.	5.4	80
177	Nanopore-confined g-C ₃ N ₄ nanodots inÂN, S co-doped hollow porous carbon with boosted capacity for lithium–sulfur batteries. Journal of Materials Chemistry A, 2018, 6, 7133-7141.	5.2	80
178	Boosting redox activity on MXene-induced multifunctional collaborative interface in high Li2S loading cathode for high-energy Li-S and metallic Li-free rechargeable batteries. Journal of Energy Chemistry, 2019, 37, 183-191.	7.1	80
179	A closed-loop and scalable process for the production of biomass-derived superhydrophilic carbon for supercapacitors. Green Chemistry, 2021, 23, 3400-3409.	4.6	80
180	Preparation of porous carbons from petroleum coke by different activation methods. Fuel, 2005, 84, 1992-1997.	3.4	79

#	Article	IF	CITATIONS
181	Highly stable lithium–sulfur batteries based on p–n heterojunctions embedded on hollow sheath carbon propelling polysulfides conversion. Journal of Materials Chemistry A, 2019, 7, 9230-9240.	5.2	79
182	Cobalt nitride nanoparticles embedded in porous carbon nanosheet arrays propelling polysulfides conversion for highly stable lithium–sulfur batteries. Energy Storage Materials, 2019, 21, 210-218.	9.5	79
183	Nitrogen and phosphorus dual-doped porous carbons for high-rate potassium ion batteries. Carbon, 2021, 179, 33-41.	5.4	79
184	Tunable full-color solid-state fluorescent carbon dots for light emitting diodes. Carbon, 2022, 190, 22-31.	5.4	79
185	Free-standing, hierarchically porous carbon nanotube film as a binder-free electrode for high-energy Li–O2 batteries. Journal of Materials Chemistry A, 2013, 1, 12033.	5.2	78
186	CoMn Layered Double Hydroxides/Carbon Nanotubes Architectures as Highâ€Performance Electrocatalysts for the Oxygen Evolution Reaction. ChemElectroChem, 2016, 3, 906-912.	1.7	78
187	Nitrogen-doped mesoporous carbon nanosheets derived from metal-organic frameworks in a molten salt medium for efficient desulfurization. Carbon, 2017, 117, 376-382.	5.4	78
188	Tuned Fabrication of the Aligned and Opened CNT Membrane with Exceptionally High Permeability and Selectivity for Bioalcohol Recovery. Nano Letters, 2018, 18, 6150-6156.	4.5	78
189	Enhancing the capacitive deionization performance of NaMnO ₂ by interface engineering and redox-reaction. Environmental Science: Nano, 2019, 6, 2379-2388.	2.2	78
190	Mutual modulation between surface chemistry and bulk microstructure within secondary particles of nickel-rich layered oxides. Nature Communications, 2020, 11, 4433.	5.8	78
191	High-purity single-wall carbon nanotubes synthesized from coal by arc discharge. Carbon, 2003, 41, 2170-2173.	5.4	77
192	Nitrogen-rich carbon coupled multifunctional metal oxide/graphene nanohybrids for long-life lithium storage and efficient oxygen reduction. Nano Energy, 2015, 12, 578-587.	8.2	76
193	Nitrogen-doped graphene nanoribbons for high-performance lithium ion batteries. Journal of Materials Chemistry A, 2014, 2, 16832-16835.	5.2	75
194	Sulfonated Graphene as Cationâ€5elective Coating: A New Strategy for Highâ€Performance Membrane Capacitive Deionization. Advanced Materials Interfaces, 2015, 2, 1500372.	1.9	75
195	In situ synthesis of super-long Cu nanowires inside carbon nanotubes with coal as carbon source. Carbon, 2006, 44, 1845-1847.	5.4	74
196	Template preparation of nanoscale CexFe1â^'xO2 solid solutions and their catalytic properties for ethanol steam reforming. Journal of Materials Chemistry, 2009, 19, 1417.	6.7	74
197	Synthesis and electrochemical performance of polyaniline–MnO2 nanowire composites for supercapacitors. Journal of Physics and Chemistry of Solids, 2013, 74, 360-365.	1.9	74
198	Organic amine-grafted carbon quantum dots with tailored surface and enhanced photoluminescence properties. Carbon, 2015, 91, 291-297.	5.4	74

#	Article	IF	CITATIONS
199	Nano-sized ZIF-8 anchored polyelectrolyte-decorated silica for Nitrogen-Rich Hollow Carbon Shell Frameworks toward alkaline and neutral supercapacitors. Carbon, 2018, 136, 176-186.	5.4	74
200	Laser Irradiation of Electrode Materials for Energy Storage and Conversion. Matter, 2020, 3, 95-126.	5.0	74
201	Three-dimensional ZnMn2O4/porous carbon framework from petroleum asphalt for high performance lithium-ion battery. Electrochimica Acta, 2015, 180, 164-172.	2.6	73
202	Synthesis of stable UiO-66 membranes for pervaporation separation of methanol/methyl tert-butyl ether mixtures by secondary growth. Journal of Membrane Science, 2017, 544, 342-350.	4.1	73
203	Preparation and gas separation properties of poly(furfuryl alcohol)-based C/CMS composite membranes. Separation and Purification Technology, 2008, 58, 412-418.	3.9	72
204	Enhancing capacitive deionization performance of electrospun activated carbon nanofibers by coupling with carbon nanotubes. Journal of Colloid and Interface Science, 2015, 446, 373-378.	5.0	72
205	Rational design and fabrication of sulfur-doped porous graphene with enhanced performance as a counter electrode in dye-sensitized solar cells. Journal of Materials Chemistry A, 2017, 5, 2280-2287.	5.2	72
206	Growth of ZnO self-converted 2D nanosheet zeolitic imidazolate framework membranes by an ammonia-assisted strategy. Nano Research, 2018, 11, 1850-1860.	5.8	72
207	A facile template-free synthesis of α-MnO2 nanorods for supercapacitor. Journal of Alloys and Compounds, 2013, 560, 151-155.	2.8	71
208	States of carbon nanotube supported Mo-based HDS catalysts. Fuel Processing Technology, 2007, 88, 117-123.	3.7	70
209	High-energy asymmetric electrochemical capacitors based on oxides functionalized hollow carbon fibers electrodes. Nano Energy, 2016, 30, 9-17.	8.2	70
210	Two-dimensional graphene-like N, Co-codoped carbon nanosheets derived from ZIF-67 polyhedrons for efficient oxygen reduction reactions. Chemical Communications, 2017, 53, 7840-7843.	2.2	70
211	Furfural-Induced Hydrothermal Synthesis of ZnO@C Gemel Hexagonal Microrods with Enhanced Photocatalytic Activity and Stability. ACS Applied Materials & Interfaces, 2014, 6, 8560-8566.	4.0	69
212	Template Preparation of Highly Active and Selective Cu–Cr Catalysts with High Surface Area for Glycerol Hydrogenolysis. Catalysis Letters, 2009, 130, 169-176.	1.4	68
213	Nitrogen-doped carbon nanotubes decorated with cobalt nanoparticles derived from zeolitic imidazolate framework-67 for highly efficient oxygen reduction reaction electrocatalysis. Carbon, 2018, 132, 580-588.	5.4	68
214	Selfâ€Templating Synthesis of 3D Hollow Tubular Porous Carbon Derived from Straw Cellulose Waste with Excellent Performance for Supercapacitors. ChemSusChem, 2019, 12, 1390-1400.	3.6	68
215	Preparation of coal-based graphene quantum dots/Î \pm -Fe2O3 nanocomposites and their lithium-ion storage properties. Fuel, 2019, 241, 646-652.	3.4	68
216	Adsorptive Removal of Thiophenic Compounds from Oils by Activated Carbon Modified with Concentrated Nitric Acid. Energy & Fuels, 2013, 27, 1499-1505.	2.5	67

#	Article	IF	CITATIONS
217	Nanogeosciences: Research History, Current Status, and Development Trends. Journal of Nanoscience and Nanotechnology, 2017, 17, 5930-5965.	0.9	67
218	ZIF-67-Derived Cobalt/Nitrogen-Doped Carbon Composites for Efficient Electrocatalytic N ₂ Reduction. ACS Applied Energy Materials, 2019, 2, 6071-6077.	2.5	67
219	High-efficient synthesis of double-walled carbon nanotubes by arc discharge method using chloride as a promoter. Carbon, 2006, 44, 516-521.	5.4	66
220	Investigating the Role of Zeolite Nanocrystal Seeds in the Synthesis of Mesoporous Catalysts with Zeolite Wall Structure. Chemistry of Materials, 2011, 23, 4469-4479.	3.2	66
221	Microwave-assisted synthesis of MoS2/graphene nanocomposites for efficient hydrodesulfurization. Fuel, 2014, 119, 163-169.	3.4	66
222	Nano-iron oxide (Fe2O3)/three-dimensional graphene aerogel composite as supercapacitor electrode materials with extremely wide working potential window. Materials Letters, 2015, 145, 44-47.	1.3	66
223	Phase controllable synthesis of Ni2+ post-modified CoP nanowire for enhanced oxygen evolution. Nano Energy, 2019, 62, 136-143.	8.2	66
224	A high CO2 permselective mesoporous silica/carbon composite membrane for CO2 separation. Carbon, 2012, 50, 5186-5195.	5.4	65
225	Au/CNTs catalyst for highly selective hydrodeoxygenation of vanillin at the water/oil interface. RSC Advances, 2014, 4, 31932-31936.	1.7	65
226	Dual integration system endowing two-dimensional titanium disulfide with enhanced triiodide reduction performance in dye-sensitized solar cells. Nano Energy, 2016, 22, 59-69.	8.2	65
227	Single-atom catalysis for electrochemical CO2 reduction. Current Opinion in Green and Sustainable Chemistry, 2019, 16, 1-6.	3.2	65
228	Low temperature plasma-mediated synthesis of graphene nanosheets for supercapacitor electrodes. Journal of Materials Chemistry, 2012, 22, 6061.	6.7	64
229	Highly controllable and green reduction of graphene oxide to flexible graphene film with high strength. Materials Research Bulletin, 2013, 48, 4797-4803.	2.7	64
230	Reduced graphene oxides with engineered defects enable efficient electrochemical reduction of dinitrogen to ammonia in wide pH range. Nano Energy, 2020, 68, 104323.	8.2	64
231	3D Carbon Frameworks for Ultrafast Charge/Discharge Rate Supercapacitors with High Energy-Power Density. Nano-Micro Letters, 2021, 13, 8.	14.4	64
232	Microscopic-Level Insights into the Mechanism of Enhanced NH ₃ Synthesis in Plasma-Enabled Cascade N ₂ Oxidation–Electroreduction System. Journal of the American Chemical Society, 2022, 144, 10193-10200.	6.6	64
233	Carbon nanofiber supported Ni catalysts for the hydrogenation of chloronitrobenzenes. Catalysis Communications, 2008, 9, 1749-1753.	1.6	63
234	Freeze-drying for sustainable synthesis of nitrogen doped porous carbon cryogel with enhanced supercapacitor and lithium ion storage performance. Nanotechnology, 2015, 26, 374003.	1.3	63

#	Article	IF	CITATIONS
235	Yellow-visual fluorescent carbon quantum dots from petroleum coke for the efficient detection of Cu2+ ions. New Carbon Materials, 2015, 30, 550-559.	2.9	63
236	Decoupling atomic-layer-deposition ultrafine RuO 2 for high-efficiency and ultralong-life Li-O 2 batteries. Nano Energy, 2017, 34, 399-407.	8.2	63
237	Molten salt synthesis of nitrogen-doped porous carbons for hydrogen sulfide adsorptive removal. Carbon, 2015, 95, 852-860.	5.4	62
238	Roles of hydrogen bonds and π–π stacking in the optical detection of nitro-explosives with a luminescent metal–organic framework as the sensor. RSC Advances, 2015, 5, 3045-3053.	1.7	62
239	Low-temperature plasma-assisted preparation of graphene supported palladium nanoparticles with high hydrodesulfurization activity. Journal of Materials Chemistry, 2012, 22, 14363.	6.7	61
240	Zeolite Married to Carbon:  A New Family of Membrane Materials with Excellent Gas Separation Performance. Chemistry of Materials, 2006, 18, 6283-6288.	3.2	60
241	Monolayer MoS2 anchored on reduced graphene oxide nanosheets for efficient hydrodesulfurization. Applied Catalysis B: Environmental, 2017, 200, 211-221.	10.8	60
242	Pickering Emulsion Catalysis: Interfacial Chemistry, Catalyst Design, Challenges, and Perspectives. Angewandte Chemie - International Edition, 2022, 61, .	7.2	60
243	Calcined MgAl-Layered Double Hydroxide/Graphene Hybrids for Capacitive Deionization. Industrial & amp; Engineering Chemistry Research, 2018, 57, 6417-6425.	1.8	59
244	Ultrafast construction of interfacial sites by wet chemical etching to enhance electrocatalytic oxygen evolution. Nano Energy, 2020, 69, 104367.	8.2	58
245	Preparation and characterization of carbon membranes made from poly(phthalazinone ether sulfone) Tj ETQq1	1 0,78431 5.4	4 rgBT /Over
246	Water-dispersible magnetic carbon nanotubes as T2-weighted MRI contrast agents. Biomaterials, 2014, 35, 378-386.	5.7	57
247	A new type of two-dimensional carbon crystal prepared from 1,3,5-trihydroxybenzene. Scientific Reports, 2017, 7, 40796.	1.6	57
248	Carbon foams produced from lignin-phenol-formaldehyde resin for oil/water separation. New Carbon Materials, 2017, 32, 86-91.	2.9	57
249	Facile Fabrication of NiCoAl-Layered Metal Oxide/Graphene Nanosheets for Efficient Capacitive Deionization Defluorination. ACS Applied Materials & amp; Interfaces, 2019, 11, 31200-31209.	4.0	57
250	Biomassâ€based Hierarchical Porous Carbon for Supercapacitors: Effect of Aqueous and Organic Electrolytes on the Electrochemical Performance. ChemSusChem, 2019, 12, 5099-5110.	3.6	57
251	Nitrogen-doped hierarchical porous carbon derived from metal–organic aerogel for high performance lithium–sulfur batteries. Journal of Energy Chemistry, 2017, 26, 1282-1290.	7.1	56
252	Promoting the electroreduction of CO ₂ with oxygen vacancies on a plasma-activated SnO _x /carbon foam monolithic electrode. Journal of Materials Chemistry A, 2020, 8, 1779-1786.	5.2	56

#	Article	IF	CITATIONS
253	Synthesis of double-walled carbon nanotubes from coal in hydrogen-free atmosphere. Fuel, 2007, 86, 282-286.	3.4	55
254	Gas separation performance of C/CMS membranes derived from poly(furfuryl alcohol) (PFA) with different chemical structure. Journal of Membrane Science, 2010, 361, 22-27.	4.1	55
255	Performance of TS-1-Coated Structured Packing Materials for Styrene Oxidation Reaction. ACS Catalysis, 2011, 1, 437-445.	5.5	55
256	New Pd/SiO ₂ @ZIF-8 Core–Shell Catalyst with Selective, Antipoisoning, and Antileaching Properties for the Hydrogenation of Alkenes. Industrial & Engineering Chemistry Research, 2014, 53, 10906-10913.	1.8	55
257	Electrochemical and Capacitive Properties of Carbon Dots/Reduced Graphene Oxide Supercapacitors. Nanomaterials, 2016, 6, 212.	1.9	55
258	Nitrogen and phosphorus dual-doped graphene as a metal-free high-efficiency electrocatalyst for triiodide reduction. Nanoscale, 2016, 8, 17458-17464.	2.8	55
259	Recognition of Water-Induced Effects toward Enhanced Interaction between Catalyst and Reactant in Alcohol Oxidation. Journal of the American Chemical Society, 2021, 143, 6071-6078.	6.6	55
260	Synthesis of a highly stable ZIF-8 membrane on a macroporous ceramic tube by manual-rubbing ZnO deposition as a multifunctional layer. Journal of Membrane Science, 2015, 490, 354-363.	4.1	54
261	Supramolecular polymerization-assisted synthesis of nitrogen and sulfur dual-doped porous graphene networks from petroleum coke as efficient metal-free electrocatalysts for the oxygen reduction reaction. Journal of Materials Chemistry A, 2017, 5, 11331-11339.	5.2	54
262	The anti-sintering catalysts: Fe–Co–Zr polymetallic fibers for CO2 hydrogenation to C2= –C4= â€ hydrocarbons. Journal of CO2 Utilization, 2018, 23, 219-225.	"rich 3.3	54
263	Fabrication of oriented metal-organic framework nanosheet membrane coated stainless steel meshes for highly efficient oil/water separation. Separation and Purification Technology, 2019, 229, 115835.	3.9	54
264	Sustainable biowaste strategy to fabricate dual-doped carbon frameworks with remarkable performance for flexible solid-state supercapacitors. Journal of Power Sources, 2019, 418, 112-121.	4.0	54
265	A Li ₂ S-based all-solid-state battery with high energy and superior safety. Science Advances, 2022, 8, eabl8390.	4.7	54
266	Effect of Na, Ca and Fe on the evolution of nitrogen species during pyrolysis and combustion of model chars. Fuel, 2003, 82, 1839-1844.	3.4	53
267	Catalytic synthesis of single-walled carbon nanotubes from coal gas by chemical vapor deposition method. Fuel Processing Technology, 2004, 85, 913-920.	3.7	53
268	Shape-Control and Characterization of Magnetite Prepared via a One-Step Solvothermal Route. Crystal Growth and Design, 2010, 10, 2863-2869.	1.4	53
269	Thermodynamically Stable Pickering Emulsion Configured with Carbon-Nanotube-Bridged Nanosheet-Shaped Layered Double Hydroxide for Selective Oxidation of Benzyl Alcohol. ACS Applied Materials & Interfaces, 2015, 7, 12203-12209.	4.0	53
270	Engineered Fabrication of Hierarchical Frameworks with Tuned Pore Structure and N,O-Co-Doping for High-Performance Supercapacitors. ACS Applied Materials & Interfaces, 2017, 9, 31940-31949.	4.0	53

#	Article	IF	CITATIONS
271	Synergies between Unsaturated Zn/Cu Doping Sites in Carbon Dots Provide New Pathways for Photocatalytic Oxidation. ACS Catalysis, 2018, 8, 747-753.	5.5	53
272	Fluorinated Polyâ€oxalate Electrolytes Stabilizing both Anode and Cathode Interfaces for Allâ€Solidâ€State Li/NMC811 Batteries. Angewandte Chemie - International Edition, 2021, 60, 18335-18343.	7.2	53
273	Boosting zinc-ion storage capability by engineering hierarchically porous nitrogen-doped carbon nanocage framework. Journal of Power Sources, 2021, 506, 230224.	4.0	53
274	Synthesis of branched carbon nanotubes from coal. Carbon, 2006, 44, 1321-1324.	5.4	52
275	Preparation and characterization of carbon and carbon/zeolite membranes from ODPA–ODA type polyetherimide. Journal of Membrane Science, 2015, 474, 114-121.	4.1	52
276	Synthesis of layered microporous carbons from coal tar by directing, space-confinement and self-sacrificed template strategy for supercapacitors. Electrochimica Acta, 2017, 246, 634-642.	2.6	52
277	Active sites-enriched carbon matrix enables efficient triiodide reduction in dye-sensitized solar cells: An understanding of the active centers. Nano Energy, 2018, 54, 138-147.	8.2	52
278	General synthesis of MXene by green etching chemistry of fluoride-free Lewis acidic melts. Rare Metals, 2020, 39, 1237-1238.	3.6	52
279	Catalytic properties of benzene hydroxylation by TS-1 film reactor and Pd–TS-1 composite membrane reactor. Catalysis Today, 2010, 156, 288-294.	2.2	51
280	Electrospun porous hierarchical carbon nanofibers with tailored structures for supercapacitors and capacitive deionization. New Journal of Chemistry, 2016, 40, 3786-3792.	1.4	51
281	A Molecularâ€Cage Strategy Enabling Efficient Chemisorption–Electrocatalytic Interface in Nanostructured Li ₂ S Cathode for Li Metalâ€Free Rechargeable Cells with High Energy. Advanced Functional Materials, 2019, 29, 1905986.	7.8	51
282	Production of carbon nanotubes from coal. Fuel Processing Technology, 2004, 85, 1663-1670.	3.7	50
283	Preparation of carbon nanofibers/carbon foam monolithic composite from coal liquefaction residue. Fuel, 2010, 89, 1169-1171.	3.4	50
284	New insights into the nitroaromatics-detection mechanism of the luminescent metal–organic framework sensor. Dalton Transactions, 2015, 44, 2897-2906.	1.6	50
285	An acid-free medium growth of rutile TiO ₂ nanorods arrays and their application in perovskite solar cells. Journal of Materials Chemistry C, 2015, 3, 729-733.	2.7	50
286	Green fabrication of magnetic recoverable graphene/MnFe ₂ O ₄ hybrids for efficient decomposition of methylene blue and the Mn/FeÂredox synergetic mechanism. RSC Advances, 2016, 6, 104549-104555.	1.7	50
287	Multifunctional nitrogen-doped graphene nanoribbon aerogels for superior lithium storage and cell culture. Nanoscale, 2016, 8, 2159-2167.	2.8	50
288	Graphene Oxide-Tuned MoS ₂ with an Expanded Interlayer for Efficient Hybrid Capacitive Deionization. ACS Sustainable Chemistry and Engineering, 2020, 8, 9690-9697.	3.2	50

#	Article	IF	CITATIONS
289	Carbon-enabled microwave chemistry: From interaction mechanisms to nanomaterial manufacturing. Nano Energy, 2021, 85, 106027.	8.2	50
290	Methanol-Mediated Electrosynthesis of Ammonia. ACS Energy Letters, 2021, 6, 3844-3850.	8.8	50
291	Influence of mineral matter in coal on decomposition of NO over coal chars and emission of NO during char combustionâ~†. Fuel, 2003, 82, 949-957.	3.4	49
292	Phaseâ€Reversal Emulsion Catalysis with CNT–TiO ₂ Nanohybrids for the Selective Oxidation of Benzyl Alcohol. Chemistry - A European Journal, 2013, 19, 16192-16195.	1.7	49
293	Preparation and gas separation performance of supported carbon membranes with ordered mesoporous carbon interlayer. Journal of Membrane Science, 2014, 450, 469-477.	4.1	49
294	Inherent N,O-containing carbon frameworks as electrode materials for high-performance supercapacitors. Nanoscale, 2016, 8, 16323-16331.	2.8	49
295	A green and template recyclable approach to prepare Fe3O4/porous carbon from petroleum asphalt for lithium-ion batteries. Journal of Alloys and Compounds, 2017, 695, 2612-2618.	2.8	49
296	Ultrasound-Assisted Nitrogen and Boron Codoping of Graphene Oxide for Efficient Oxygen Reduction Reaction. ACS Sustainable Chemistry and Engineering, 2019, 7, 3434-3442.	3.2	49
297	A durable MXene-based zinc ion hybrid supercapacitor with sulfated polysaccharide reinforced hydrogel/electrolyte. Journal of Materials Chemistry A, 2021, 9, 23941-23954.	5.2	49
298	A novel carbon/ZSM-5 nanocomposite membrane with high performance for oxygen/nitrogen separation. Chemical Communications, 2006, , 1230.	2.2	48
299	A general strategy for synthesis of silver dendrites by galvanic displacement under hydrothermal conditions. Journal of Physics and Chemistry of Solids, 2008, 69, 1296-1300.	1.9	48
300	Preparation of carbon microfibers from coal liquefaction residue. Fuel, 2008, 87, 3474-3476.	3.4	48
301	An Aerobic and Very Fast Pd/C atalyzed Ligandâ€Free and Aqueous Suzuki Reaction Under Mild Conditions. European Journal of Organic Chemistry, 2013, 2013, 4345-4350.	1.2	48
302	Magnetically recoverable Ni/C catalysts with hierarchical structure and high-stability for selective hydrogenation of nitroarenes. Physical Chemistry Chemical Physics, 2015, 17, 145-150.	1.3	48
303	Ultrahighâ€Capacity and Longâ€Life Lithium–Metal Batteries Enabled by Engineering Carbon Nanofiber–Stabilized Graphene Aerogel Film Host. Small, 2018, 14, e1803310.	5.2	48
304	Strategies to activate inert nitrogen molecules for efficient ammonia electrosynthesis: current status, challenges, and perspectives. Energy and Environmental Science, 2022, 15, 2776-2805.	15.6	48
305	Core–shell Pd/ZSM-5@ZIF-8 membrane micro-reactors with size selectivity properties for alkene hydrogenation. Catalysis Today, 2014, 236, 41-48.	2.2	47
306	Solvent engineering of spin-coating solutions for planar-structured high-efficiency perovskite solar cells. Chinese Journal of Catalysis, 2015, 36, 1183-1190.	6.9	47

#	Article	IF	CITATIONS
307	Towards efficient electrocatalysts for oxygen reduction by doping cobalt into graphene-supported graphitic carbon nitride. Journal of Materials Chemistry A, 2015, 3, 19657-19661.	5.2	47
308	Surface-to-Bulk Redox Coupling through Thermally Driven Li Redistribution in Li- and Mn-Rich Layered Cathode Materials. Journal of the American Chemical Society, 2019, 141, 12079-12086.	6.6	47
309	Flowing nitrogen assisted-arc discharge synthesis of nitrogen-doped single-walled carbon nanohorns. Applied Surface Science, 2013, 277, 88-93.	3.1	46
310	Polymer casting of ultralight graphene aerogels for the production of conductive nanocomposites with low filling content. Journal of Materials Chemistry A, 2014, 2, 3756-3760.	5.2	46
311	Graphene oxide liquid crystal Pickering emulsions and their assemblies. Carbon, 2015, 85, 16-23.	5.4	46
312	Efficient visible-light driven N ₂ fixation over two-dimensional Sb/TiO ₂ composites. Chemical Communications, 2019, 55, 7171-7174.	2.2	46
313	Microwaveâ€Assisted Ultrafast Synthesis of Molybdenum Carbide Nanoparticles Grown on Carbon Matrix for Efficient Hydrogen Evolution Reaction. Small Methods, 2019, 3, 1900259.	4.6	46
314	Electrochemically Driven Coordination Tuning of FeOOH Integrated on Carbon Fiber Paper for Enhanced Oxygen Evolution. Small, 2019, 15, e1901015.	5.2	46
315	Preparation and performance of TS-1/SiO2 egg-shell catalysts. Chemical Engineering Journal, 2011, 175, 408-416.	6.6	45
316	Novel triphenylamine-based cyclometalated platinum(II) complexes for efficient luminescent oxygen sensing. Dyes and Pigments, 2014, 101, 85-92.	2.0	45
317	Achieving ultralong life sodium storage in amorphous cobalt–tin binary sulfide nanoboxes sheathed in N-doped carbon. Journal of Materials Chemistry A, 2017, 5, 10398-10405.	5.2	45
318	Coal gasification in steam and air medium under plasma conditions: a preliminary study. Fuel Processing Technology, 2004, 85, 969-982.	3.7	44
319	Structure and morphology of microporous carbon membrane materials derived from poly(phthalazinone ether sulfone ketone). Microporous and Mesoporous Materials, 2006, 96, 79-83.	2.2	44
320	Preparation of double-walled carbon nanotubes from fullerene waste soot by arc-discharge. Carbon, 2010, 48, 1312-1315.	5.4	44
321	Trifluoromethyl-substituted cyclometalated iridium ^{III} emitters with high photostability for continuous oxygen sensing. Journal of Materials Chemistry C, 2015, 3, 8010-8017.	2.7	44
322	Ultrasmall diiron phosphide nanodots anchored on graphene sheets with enhanced electrocatalytic activity for hydrogen production via high-efficiency water splitting. Journal of Materials Chemistry A, 2016, 4, 16028-16035.	5.2	44
323	In situ synthesis of cotton-derived Ni/C catalysts with controllable structures and enhanced catalytic performance. Green Chemistry, 2016, 18, 3594-3599.	4.6	44
324	Moss-Covered Rock-like Hybrid Porous Carbons with Enhanced Electrochemical Properties. ACS Sustainable Chemistry and Engineering, 2020, 8, 3065-3071.	3.2	44

#	Article	IF	CITATIONS
325	Operando Tailoring of Defects and Strains in Corrugated βâ€Ni(OH) ₂ Nanosheets for Stable and Highâ€Rate Energy Storage. Advanced Materials, 2021, 33, e2006147.	11.1	44
326	Influence of KOH/Coke Mass Ratio on Properties of Activated Carbons Made by Microwave-Assisted Activation for Electric Double-Layer Capacitors. Energy & Fuels, 2010, 24, 3603-3609.	2.5	43
327	Facile synthesis of highly graphitized porous carbon monoliths with a balance on crystallization and pore-structure. Journal of Materials Chemistry A, 2014, 2, 12785-12791.	5.2	43
328	One-step synthesis of flowerlike C/Fe2O3 nanosheet assembly with superior adsorption capacity and visible light photocatalytic performance for dye removal. Carbon, 2017, 116, 59-67.	5.4	43
329	Crumpled carbon nanonets derived from anthracene oil for high energy density supercapacitor. Journal of Power Sources, 2019, 428, 8-12.	4.0	43
330	Interconnected N/P co-doped carbon nanocage as high capacitance electrode material for energy storage devices. Nano Research, 2022, 15, 4068-4075.	5.8	43
331	Synthesis of carbon-encapsulated nickel nanocrystals by arc-discharge of coal-based carbons in water. Fuel, 2004, 83, 615-617.	3.4	42
332	Effect of carbonization atmosphere on the structure changes of PAN carbon membranes. Journal of Porous Materials, 2009, 16, 197-203.	1.3	42
333	Carbon foams made of in situ produced carbon nanocapsules and the use as a catalyst for oxidative dehydrogenation of ethylbenzene. Carbon, 2013, 60, 514-522.	5.4	42
334	Investigation of SO2 gas adsorption in metal–organic frameworks by molecular simulation. Inorganic Chemistry Communication, 2014, 46, 277-281.	1.8	42
335	Capping nanoparticles with graphene quantum dots for enhanced thermoelectric performance. Chemical Science, 2015, 6, 4103-4108.	3.7	42
336	TiO2 quantum dots embedded in bamboo-like porous carbon nanotubes as ultra high power and long life anodes for lithium ion batteries. Journal of Power Sources, 2016, 319, 227-234.	4.0	42
337	Mismatching integration-enabled strains and defects engineering in LDH microstructure for high-rate and long-life charge storage. Nature Communications, 2022, 13, 1409.	5.8	42
338	Controlled synthesis of high performance carbon/zeolite T composite membrane materials for gas separation. Microporous and Mesoporous Materials, 2009, 120, 460-466.	2.2	41
339	Effects of sulfone/ketone in poly(phthalazinone ether sulfone ketone) on the gas permeation of their derived carbon membranes. Journal of Membrane Science, 2009, 330, 319-325.	4.1	41
340	Electrolysis removal of methyl orange dye from water by electrospun activated carbon fibers modified with carbon nanotubes. Chemical Engineering Journal, 2014, 253, 73-77.	6.6	41
341	Catalytic role of β-Mo2C in DRM catalysts that contain Ni and Mo. Catalysis Today, 2015, 258, 676-683.	2.2	41
342	Nitrogen-doped tubular carbon foam electrodes for efficient electroreduction of CO ₂ to syngas with potential-independent CO/H ₂ ratios. Journal of Materials Chemistry A, 2019, 7, 18852-18860.	5.2	41

#	Article	IF	CITATIONS
343	3D nanoflower-like composite anode of α-Fe2O3/coal-based graphene for lithium-ion batteries. Journal of Alloys and Compounds, 2019, 792, 828-834.	2.8	41
344	A Câ€S Linkageâ€Triggered Ultrahigh Nitrogenâ€Doped Carbon and the Identification of Active Site in Triiodide Reduction. Angewandte Chemie - International Edition, 2021, 60, 3587-3595.	7.2	41
345	Hydrogenâ€Bonding Crosslinking MXene to Highly Robust and Ultralight Aerogels for Strengthening Lithium Metal Anode. Small Science, 2021, 1, 2100021.	5.8	41
346	Three-dimensional hierarchical Na3Fe2(PO4)3/C with superior and fast sodium uptake for efficient hybrid capacitive deionization. Desalination, 2021, 520, 115341.	4.0	41
347	Synthesis and structure regulation of armor-wearing biomass-based porous carbon: Suppression the leakage current and self-discharge of supercapacitors. Carbon, 2022, 196, 136-145.	5.4	41
348	Selective hydrogenation of cinnamaldehyde over carbon nanotube supported pd-ru catalyst. Reaction Kinetics and Catalysis Letters, 2006, 88, 269-276.	0.6	40
349	Synergism in NiMoOx precursors essential for CH4/CO2 dry reforming. Catalysis Today, 2014, 233, 46-52.	2.2	40
350	Electrospun nitrogen-doped carbon nanofibers with tuned microstructure and enhanced lithium storage properties. Carbon, 2018, 139, 716-724.	5.4	40
351	Efficient Electrochemical Reduction of CO ₂ by Ni–N Catalysts with Tunable Performance. ACS Sustainable Chemistry and Engineering, 2019, 7, 15030-15035.	3.2	40
352	A quasi-solid-state rechargeable cell with high energy and superior safety enabled by stable redox chemistry of Li ₂ S in gel electrolyte. Energy and Environmental Science, 2021, 14, 2278-2290.	15.6	40
353	A General and Highly Efficient Method for the Construction of Arylâ€Substituted Nâ€Heteroarenes. European Journal of Organic Chemistry, 2010, 2010, 5548-5551.	1.2	39
354	A quinoline-functionalized amphiphilic fluorogenic probe for specific detection of trivalent cations. RSC Advances, 2014, 4, 46955-46961.	1.7	39
355	Hybrid pseudocapacitor materials from polyaniline@multi-walled carbon nanotube with ultrafine nanofiber-assembled network shell. Carbon, 2015, 95, 323-329.	5.4	39
356	Self-assembled sulfur/reduced graphene oxide nanoribbon paper as a free-standing electrode for high performance lithium–sulfur batteries. Chemical Communications, 2016, 52, 12825-12828.	2.2	39
357	Metal-Tuned W ₁₈ O ₄₉ for Efficient Electrocatalytic N ₂ Reduction. ACS Sustainable Chemistry and Engineering, 2020, 8, 2957-2963.	3.2	39
358	A multi-interface CoNi-SP/C heterostructure for quasi-solid-state hybrid supercapacitors with a graphene oxide-containing hydrogel electrolyte. Journal of Materials Chemistry A, 2022, 10, 4671-4682.	5.2	39
359	Preparation of core (Ni base)–shell (Silicalite-1) catalysts and their application for alkali resistance in direct internal reforming molten carbonate fuel cell. Journal of Power Sources, 2012, 198, 14-22.	4.0	38
360	Biomass-Derived Carbon Nanospheres with Turbostratic Structure as Metal-Free Catalysts for Selective Hydrogenation of <i>o</i> -Chloronitrobenzene. ACS Sustainable Chemistry and Engineering, 2017, 5, 7481-7485.	3.2	38

#	Article	IF	CITATIONS
361	High performance concentration capacitors with graphene hydrogel electrodes for harvesting salinity gradient energy. Journal of Materials Chemistry A, 2018, 6, 4981-4987.	5.2	38
362	Carbon clusters decorated hard carbon nanofibers as high-rate anode material for lithium-ion batteries. Fuel Processing Technology, 2018, 180, 173-179.	3.7	38
363	Scalable synthesis of 2D hydrogen-substituted graphdiyne on Zn substrate for high-yield N2 fixation. Nano Energy, 2020, 78, 105283.	8.2	38
364	Full Bulk‧tructure Reconstruction into Amorphorized Cobalt–Iron Oxyhydroxide Nanosheet Electrocatalysts for Greatly Improved Electrocatalytic Activity. Small Methods, 2020, 4, 2000546.	4.6	38
365	Factors affecting the formation of Sn-Beta zeolites by steam-assisted conversion method. Materials Chemistry and Physics, 2013, 141, 519-529.	2.0	37
366	Effective thermodynamic alteration to Mg(NH ₂) ₂ –LiH system: achieving near ambient-temperature hydrogen storage. Journal of Materials Chemistry A, 2014, 2, 15816-15822.	5.2	37
367	An effective graphene confined strategy to construct active edge sites-enriched nanosheets with enhanced oxygen evolution. Carbon, 2018, 126, 437-442.	5.4	37
368	Surface-engineered oxidized two-dimensional Sb for efficient visible light-driven N2 fixation. Nano Energy, 2020, 78, 105368.	8.2	37
369	Insights into the Anchoring of Polysulfides and Catalytic Performance by Metal Phthalocyanine Covalent Organic Frameworks as the Cathode in Lithium–Sulfur Batteries. ACS Sustainable Chemistry and Engineering, 2020, 8, 10185-10192.	3.2	37
370	Timeâ€dependent density functional theory study on the electronic excitedâ€state hydrogenâ€bonding dynamics of 4â€aminophthalimide (4AP) in aqueous solution: 4AP and 4AP–(H ₂ O) _{1,2} clusters. Journal of Computational Chemistry, 2010, 31, 2157-2163.	1.5	36
371	Effects of excited-state structures and properties on photochemical degradation of polybrominated diphenyl ethers: A TDDFT study. Chemosphere, 2012, 88, 33-38.	4.2	36
372	Pd nanoparticles immobilized in a microporous/mesoporous composite ZIF-8/MSS: A multifunctional catalyst for the hydrogenation of alkenes. Microporous and Mesoporous Materials, 2014, 197, 324-330.	2.2	36
373	Interaction between Formaldehyde and Luminescent MOF [Zn(NH ₂ bdc)(bix)] _{<i>n</i>} in the Electronic Excited State. Journal of Physical Chemistry A, 2014, 118, 6191-6196.	1.1	36
374	Ultrasmall MoS 2 Nanosheets Mosaiced into Nitrogen-Doped Hierarchical Porous Carbon Matrix for Enhanced Sodium Storage Performance. Electrochimica Acta, 2017, 225, 369-377.	2.6	36
375	Toward an Understanding of the Enhanced CO ₂ Electroreduction in NaCl Electrolyte over CoPc Moleculeâ€implanted Graphitic Carbon Nitride Catalyst. Advanced Energy Materials, 2021, 11, 2100075.	10.2	36
376	Core-Shell ZIF-67@ZIF-8-derived multi-dimensional cobalt-nitrogen doped hierarchical carbon nanomaterial for efficient oxygen reduction reaction. Journal of Alloys and Compounds, 2022, 903, 163701.	2.8	36
377	A novel approach for the preparation of highly stable Pd membrane on macroporous α-Al2O3 tube. Journal of Membrane Science, 2010, 362, 241-248.	4.1	35
378	An active and coke-resistant dry reforming catalyst comprising nickel–tungsten alloy nanoparticles. Catalysis Communications, 2015, 69, 123-128.	1.6	35

#	Article	lF	CITATIONS
379	Polystyrene sphere-mediated ultrathin graphene sheet-assembled frameworks for high-power density Li–O ₂ batteries. Chemical Communications, 2015, 51, 13233-13236.	2.2	35
380	NiWO4/Ni/Carbon Composite Fibres for Supercapacitors with Excellent Cycling Performance. Electrochimica Acta, 2016, 222, 446-454.	2.6	35
381	Targeted Fe-filled carbon nanotube as a multifunctional contrast agent for thermoacoustic and magnetic resonance imaging of tumor in living mice. Nanomedicine: Nanotechnology, Biology, and Medicine, 2016, 12, 235-244.	1.7	35
382	Pt/ZnO@C Nanocable with Dual-Enhanced Photocatalytic Performance and Superior Photostability. Langmuir, 2017, 33, 4452-4460.	1.6	35
383	Interface Engineering of Ni ₃ N@Fe ₃ N Heterostructure Supported on Carbon Fiber for Enhanced Water Oxidation. Industrial & Engineering Chemistry Research, 2017, 56, 14245-14251.	1.8	35
384	Wrinkled porous carbon nanosheets from methylnaphthalene oil for high-performance supercapacitors. Fuel Processing Technology, 2018, 175, 10-16.	3.7	35
385	New Insights into the Anchoring Mechanism of Polysulfides inside Nanoporous Covalent Organic Frameworks for Lithium–Sulfur Batteries. ACS Applied Materials & Interfaces, 2018, 10, 43896-43903.	4.0	35
386	Polyethyleneimine-Mediated Fabrication of Two-Dimensional Cobalt Sulfide/Graphene Hybrid Nanosheets for High-Performance Supercapacitors. ACS Applied Materials & Interfaces, 2019, 11, 26235-26242.	4.0	35
387	Synthesis, modification strategies and applications of coal-based carbon materials. Fuel Processing Technology, 2022, 230, 107203.	3.7	35
388	Catalytic effect of Na–Fe on NO–char reaction and NO emission during coal char combustion. Fuel, 2002, 81, 2343-2348.	3.4	34
389	Preparation of carbon-coated magnetic iron nanoparticles from composite rods made from coal and iron powders. Fuel Processing Technology, 2004, 86, 267-274.	3.7	34
390	Effects of carbonization conditions on the properties of coal-based microfiltration carbon membranes. Journal of Porous Materials, 2008, 15, 1-6.	1.3	34
391	Preparation and gas permeation of composite carbon membranes from poly(phthalazinone ether) Tj ETQq1 1 0.7	84314 rg8 3.9	3T /Overlock
392	Influence of pore structures on the electrochemical performance of asphaltene-based ordered mesoporous carbons. Microporous and Mesoporous Materials, 2013, 174, 67-73.	2.2	34
393	Implanting CNT Forest onto Carbon Nanosheets as Multifunctional Hosts for Highâ€Performance Lithium Metal Batteries. Small Methods, 2019, 3, 1800546.	4.6	34
394	A new approach to high performance Co/C catalysts for selective hydrogenation of chloronitrobenzenes. Journal of Catalysis, 2007, 250, 369-372.	3.1	33
395	H _x MoO _{3â^'y} nanobelts with sea water as electrolyte for high-performance pseudocapacitors and desalination devices. Journal of Materials Chemistry A, 2015, 3, 17217-17223.	5.2	33
396	Tailor-made graphene aerogels with inbuilt baffle plates by charge-induced template-directed assembly for high-performance Li–S batteries. Journal of Materials Chemistry A, 2015, 3, 21842-21848.	5.2	33

#	Article	IF	CITATIONS
397	Ternary NiFeMn layered metal oxide (LDO) compounds for capacitive deionization defluoridation: The unique role of Mn. Separation and Purification Technology, 2021, 254, 117667.	3.9	33
398	Thermal-healing of lattice defects for high-energy single-crystalline battery cathodes. Nature Communications, 2022, 13, 704.	5.8	33
399	In situ formation of N,O-bidentate ligand via the hydrogen bond for highly efficient Suzuki reaction of aryl chlorides. Chemical Communications, 2010, 46, 2659.	2.2	32
400	Novel hydrodesulfurization nano-catalysts derived from Co3O4 nanocrystals with different shapes. Catalysis Today, 2011, 175, 509-514.	2.2	32
401	Chemically patterned polyaniline arrays located on pyrolytic graphene for supercapacitors. Carbon, 2014, 80, 799-807.	5.4	32
402	In situ fabrication of high-permeance ZIF-8 tubular membranes in a continuous flow system. Materials Chemistry and Physics, 2014, 148, 10-16.	2.0	32
403	Compressible graphene aerogel supported CoO nanostructures as a binder-free electrode for high-performance lithium-ion batteries. RSC Advances, 2015, 5, 8929-8932.	1.7	32
404	Ultrafine Fe ₃ O ₄ Quantum Dots on Hybrid Carbon Nanosheets for Longâ€Life, Highâ€Rate Alkaliâ€Metal Storage. ChemElectroChem, 2016, 3, 38-44.	1.7	32
405	CoS nanosheets-coupled graphene quantum dots architectures as a binder-free counter electrode for high-performance DSSCs. Science China Materials, 2016, 59, 104-111.	3.5	32
406	Nitrogen-doped tubular/porous carbon channels implanted on graphene frameworks for multiple confinement of sulfur and polysulfides. Journal of Materials Chemistry A, 2017, 5, 10380-10386.	5.2	32
407	Ultrathin Nitrogenâ€Enriched Hybrid Carbon Nanosheets for Supercapacitors with Ultrahigh Rate Performance and High Energy Density. ChemElectroChem, 2017, 4, 369-375.	1.7	32
408	Preparation and characterization of a diatomite hybrid microfiltration carbon membrane for oily wastewater treatment. Journal of the Taiwan Institute of Chemical Engineers, 2018, 89, 39-48.	2.7	32
409	Covalent bonds-integrated graphene foam with superb electromechanical properties as elastic conductor and compressive sensor. Carbon, 2019, 147, 206-213.	5.4	32
410	Nitrogen-rich hierarchical porous carbon nanofibers for selective oxidation of hydrogen sulfide. Fuel Processing Technology, 2019, 191, 121-128.	3.7	32
411	Oriented Nanosheet-Assembled CoNi-LDH Cages with Efficient Ion Diffusion for Quasi-Solid-State Hybrid Supercapacitors. Inorganic Chemistry, 2021, 60, 12197-12205.	1.9	32
412	An ionic liquid template approach to graphene–carbon xerogel composites for supercapacitors with enhanced performance. Journal of Materials Chemistry A, 2014, 2, 14329.	5.2	31
413	General synthesis of zeolitic imidazolate framework-derived planar-N-doped porous carbon nanosheets for efficient oxygen reduction. Energy Storage Materials, 2017, 7, 181-188.	9.5	31
414	High performance asymmetric capacitive mixing with oppositely charged carbon electrodes for energy production from salinity differences. Journal of Materials Chemistry A, 2017, 5, 20374-20380.	5.2	31

#	Article	IF	CITATIONS
415	Nanogeology in China: A review. China Geology, 2018, 1, 286-303.	0.5	31
416	Inverted Capacitive Deionization with Highly Enhanced Stability Performance Utilizing Ionic Liquid-Functionalized Carbon Electrodes. ACS Sustainable Chemistry and Engineering, 2019, 7, 15715-15722.	3.2	31
417	Boron-nitride-carbon nanosheets with different pore structure and surface properties for capacitive deionization. Journal of Colloid and Interface Science, 2019, 552, 604-612.	5.0	31
418	Designed synthesis of cobalt nanoparticles embedded carbon nanocages as bifunctional electrocatalysts for oxygen evolution and reduction. Carbon, 2019, 144, 492-499.	5.4	31
419	Rational design of metal oxide hollow nanostructures decorated carbon nanosheets for superior lithium storage. Journal of Materials Chemistry A, 2016, 4, 17718-17725.	5.2	30
420	Boosting charge storage in 1D manganese oxide-carbon composite by phosphorus-assisted structural modification for supercapacitor applications. Energy Storage Materials, 2020, 31, 172-180.	9.5	30
421	Carbon Nanotube Templated Synthesis of CeF3 Nanowires. Chemistry of Materials, 2007, 19, 3364-3366.	3.2	29
422	Microwave-Assisted Preparation and Hydrazine Decomposition Properties of Nanostructured Tungsten Carbides on Carbon Nanotubes. Industrial & Engineering Chemistry Research, 2009, 48, 3244-3248.	1.8	29
423	A highly efficient and aerobic protocol for the synthesis of N-heteroaryl substituted 9-arylcarbazolyl derivatives via a palladium-catalyzed ligand-free Suzuki reaction. Organic and Biomolecular Chemistry, 2012, 10, 7875.	1.5	29
424	Nitrogen-doped carbon microfibers with porous textures. Carbon, 2013, 58, 128-133.	5.4	29
425	Phosphate Species up to 70% Mass Ratio for Enhanced Pseudocapacitive Properties. Small, 2018, 14, e1803811.	5.2	29
426	Polyvinyl pyrrolidone mediated fabrication of Fe, N-codoped porous carbon sheets for efficient electrocatalytic CO2 reduction. Carbon, 2019, 153, 609-616.	5.4	29
427	Insights into the electronic origin of enhancing the catalytic activity of Co3O4 for oxygen evolution by single atom ruthenium. Nano Today, 2020, 34, 100955.	6.2	29
428	A novel approach to Co/CNTs catalyst via chemical vapor deposition of organometallic compounds. Catalysis Letters, 2005, 101, 211-214.	1.4	28
429	Co/CNF Catalysts Tailored by Controlling the Deposition of Metal Colloids onto CNFs: Preparation and Catalytic Properties. Chemistry - A European Journal, 2006, 12, 2147-2151.	1.7	28
430	Hierarchical Hybrids Integrated by Dual Polypyrroleâ€Based Porous Carbons for Enhanced Capacitive Performance. Chemistry - A European Journal, 2017, 23, 13474-13481.	1.7	28
431	In situ synthesis of chemically active ZIF coordinated with electrospun fibrous film for heavy metal removal with a high flux. Separation and Purification Technology, 2017, 177, 257-262.	3.9	28
432	Scrutinizing Defects and Defect Density of Seleniumâ€Doped Graphene for Highâ€Efficiency Triiodide Reduction in Dyeâ€Sensitized Solar Cells. Angewandte Chemie, 2018, 130, 4772-4776.	1.6	28

#	Article	IF	CITATIONS
433	Liquid Exfoliation of Two-Dimensional PbI ₂ Nanosheets for Ultrafast Photonics. ACS Photonics, 2019, 6, 1051-1057.	3.2	28
434	A long/short-range interconnected carbon with well-defined mesopore for high-energy-density supercapacitors. Nano Research, 2022, 15, 1399-1408.	5.8	28
435	Thermal conductivity of a single carbon nanocoil measured by field-emission induced thermal radiation. Carbon, 2012, 50, 778-783.	5.4	27
436	Palladium-catalyzed ligand-free and aqueous Suzuki reaction for the construction of (hetero)aryl-substituted triphenylamine derivatives. RSC Advances, 2013, 3, 526-531.	1.7	27
437	Effects of Al-based additives on the hydrogen storage performance of the Mg(NH2)2–2LiH system. Dalton Transactions, 2013, 42, 5524.	1.6	27
438	Synthesis of metallic Ni-Co/graphene catalysts with enhanced hydrodesulfurization activity via a low-temperature plasma approach. Catalysis Today, 2015, 256, 203-208.	2.2	27
439	Modification of the desalination property of PAN-based nanofiltration membranes by a preoxidation method. Desalination, 2015, 357, 208-214.	4.0	27
440	Porous polyaniline arrays oriented on functionalized carbon cloth as binder-free electrode for flexible supercapacitors. Journal of Electroanalytical Chemistry, 2019, 848, 113348.	1.9	27
441	A new alkali-resistant Ni/Al2O3-MSU-1 core–shell catalyst for methane steam reforming in a direct internal reforming molten carbonate fuel cell. Journal of Power Sources, 2014, 246, 74-83.	4.0	26
442	Long life rechargeable Li-O2 batteries enabled by enhanced charge transfer in nanocable-like Fe@N-doped carbon nanotube catalyst. Science China Materials, 2017, 60, 415-426.	3.5	26
443	High-Performance Co-Based ZIF-67 Tubular Membrane Achieved by ZnO-Induced Synthesis for Highly Efficient Pervaporation Separation of Methanol/Methyl <i>tert</i> Butyl Ether Mixture. Industrial & Engineering Chemistry Research, 2019, 58, 15297-15306.	1.8	26
444	Activated coal-based graphene with hierarchical porous structures for ultra-high energy density supercapacitors. Diamond and Related Materials, 2020, 106, 107827.	1.8	26
445	Very Fast, Ligandâ€Free and Aerobic Protocol for the Synthesis of 4â€Arylâ€Substituted Triphenylamine Derivatives. European Journal of Organic Chemistry, 2011, 2011, 3009-3015.	1.2	25
446	Facile hydrothermal synthesis of SnO2/C microspheres and double layered core–shell SnO2 microspheres as anode materials for Li-ion secondary batteries. RSC Advances, 2014, 4, 25189-25194.	1.7	25
447	Improved kinetics of the Mg(NH ₂) ₂ –2LiH system by addition of lithium halides. RSC Advances, 2014, 4, 32555.	1.7	25
448	NH ₃ Mediated or Ion Migration Reaction: The Case Study on Halide–Amide System. Journal of Physical Chemistry C, 2014, 118, 2344-2349.	1.5	25
449	Facile Fabrication of Bicomponent CoO/CoFe ₂ O ₄ â€Nâ€Doped Graphene Hybrids with Ultrahigh Lithium Storage Capacity. Particle and Particle Systems Characterization, 2015, 32, 91-97.	1.2	25
450	In-situ growth of highly uniform and single crystalline Co3O4 nanocubes on graphene for efficient oxygen evolution. Catalysis Communications, 2017, 88, 81-84.	1.6	25

#	Article	IF	CITATIONS
451	Triphenylamine-modified difluoroboron dibenzoylmethane derivatives: Synthesis, photophysical and electrochemical properties. Dyes and Pigments, 2017, 136, 798-806.	2.0	25
452	Boosting the sodium storage performance of coal-based carbon materials through structure modification by solvent extraction. Carbon, 2020, 162, 431-437.	5.4	25
453	Facile synthesis of low-cost MnPO4 with hollow grape-like clusters for rapid removal uranium from wastewater. Journal of Hazardous Materials, 2022, 434, 128894.	6.5	25
454	Synthesis of nanostructured ceria, zirconia and ceria–zirconia solid solutions using an ultrahigh surface area carbon material as a template. Nanotechnology, 2004, 15, 843-847.	1.3	24
455	Increasing the shell thickness by controlling the core size of zeolite capsule catalyst: Application in iso-paraffin direct synthesis. Catalysis Communications, 2008, 9, 2520-2524.	1.6	24
456	Investigation of Pd membrane reactors for one-step hydroxylation of benzene to phenol. Catalysis Today, 2012, 193, 151-157.	2.2	24
457	A time-dependent density functional theory study on the effect of electronic excited-state hydrogen bonding on luminescent MOFs. Dalton Transactions, 2013, 42, 3464-3470.	1.6	24
458	Ionic liquid as template to synthesize carbon xerogels by coupling with KOH activation for supercapacitors. Electrochemistry Communications, 2013, 31, 31-34.	2.3	24
459	Synthesis and characterization of ZIF-8@SiO2@Fe3O4 core@double-shell microspheres with noble metal nanoparticles sandwiched between two shell layers. Materials Letters, 2015, 148, 17-21.	1.3	24
460	Biomimetic Preparation of Hybrid Porous Adsorbents for Efficiently Purifying Complex Wastewater. ACS Sustainable Chemistry and Engineering, 2016, 4, 992-998.	3.2	24
461	A General Surface Swellingâ€Induced Electroless Deposition Strategy for Fast Fabrication of Copper Circuits on Various Polymer Substrates. Advanced Materials Interfaces, 2017, 4, 1700052.	1.9	24
462	From fluorene molecules to ultrathin carbon nanonets with an enhanced charge transfer capability for supercapacitors. Nanoscale, 2019, 11, 6610-6619.	2.8	24
463	Effective Fixation of Carbon in g ₃ N ₄ Enabled by Mgâ€Induced Selective Reconstruction. Small, 2020, 16, e1907164.	5.2	24
464	Microstructure regulation of pitch-based soft carbon anodes by iodine treatment towards high-performance potassium-ion batteries. Journal of Colloid and Interface Science, 2022, 615, 485-493.	5.0	24
465	Sodium Metal Anodes with Selfâ€Correction Function Based on Fluorineâ€5uperdoped CNTs/Cellulose Nanofibrils Composite Paper. Advanced Functional Materials, 2022, 32, .	7.8	24
466	Water-assisted fabrication of aligned microsized carbon tubes made of self-assembled multi-wall carbon nanotubes. Chemical Communications, 2006, , 594-596.	2.2	23
467	A recyclable route to produce biochar with a tailored structure and surface chemistry for enhanced charge storage. Green Chemistry, 2019, 21, 2095-2103.	4.6	23
468	Engineering Kinetics-Favorable Carbon Sheets with an Intrinsic Network for a Superior Supercapacitor Containing a Dual Cross-linked Hydrogel Electrolyte. ACS Applied Materials & Interfaces, 2020, 12, 53164-53173.	4.0	23

#	Article	IF	CITATIONS
469	3D hierarchical carbons composed of cross-linked porous carbon nanosheets for supercapacitors. Journal of Power Sources, 2020, 474, 228698.	4.0	23
470	Bimetallic Zn/Co-ZIF tubular membrane for highly efficient pervaporation separation of Methanol/MTBE mixture. Journal of Membrane Science, 2021, 638, 119676.	4.1	23
471	Ni@Ni ₃ N Embedded on Three-Dimensional Carbon Nanosheets for High-Performance Lithium/Sodium–Sulfur Batteries. ACS Applied Materials & Interfaces, 2021, 13, 48536-48545.	4.0	23
472	Molecular tuning of sulfur doped quinoline oligomer derived soft carbon for superior potassium storage. Carbon, 2022, 191, 10-18.	5.4	23
473	Hydrogen Production and Water Desalination with Onâ€demand Electricity Output Enabled by Electrochemical Neutralization Chemistry. Angewandte Chemie - International Edition, 2022, 61, .	7.2	23
474	Preparation and Characterization of Carbon Membranes Derived from Poly(phthalazinone ether) Tj ETQq0 0 0 rg	;BT/Qverlc 1.8	აck_10 Tf 50 5 22
475	Zeolite capillary microreactor by flow synthesis method. Catalysis Today, 2012, 193, 221-225.	2.2	22

Nitrogen-doped mesoporous carbon nanosheets from coal tar as high performance anode materials for lithium ion batteries. New Carbon Materials, 2014, 29, 280-286. 476 2.9 22

477	Phosphorus Removal from Silicon by Vacuum Refining and Directional Solidification. Journal of Electronic Materials, 2014, 43, 314-319.	1.0	22
478	Monolithic coal-based carbon counter electrodes for highly efficient dye-sensitized solar cells. Carbon, 2014, 67, 465-474.	5.4	22
479	Theoretical investigation on photodechlorination mechanism of polychlorinated biphenyls. Chemosphere, 2014, 95, 200-205.	4.2	22
480	Hierarchically porous carbon architectures embedded with hollow nanocapsules for high-performance lithium storage. Journal of Materials Chemistry A, 2015, 3, 5054-5059.	5.2	22
481	A hydrogel-mediated scalable strategy toward core-shell polyaniline/poly(acrylic acid)-modified carbon nanotube hybrids as efficient electrodes for supercapacitor applications. Applied Surface Science, 2018, 436, 189-197.	3.1	22
482	Operando leaching of pre-incorporated Al and mechanism in transition-metal hybrids on carbon substrates for enhanced charge storage. Matter, 2021, 4, 2902-2918.	5.0	22
483	NiCo (oxy)selenide electrocatalysts <i>via</i> anionic regulation for high-performance lithium–sulfur batteries. Journal of Materials Chemistry A, 2022, 10, 5410-5419.	5.2	22
484	Ultraâ€High Fluorine Enhanced Homogeneous Nucleation of Lithium Metal on Stepped Carbon Nanosheets with Abundant Edge Sites. Advanced Energy Materials, 2022, 12, .	10.2	22
485	Fabrication of ZnO microtube arrays via vapor phase growth. Materials Letters, 2008, 62, 1528-1531.	1.3	21
486	KOH-activated depleted fullerene soot for electrochemical double-layer capacitors. Journal of Applied Electrochemistry, 2014, 44, 309-316.	1.5	21

KOH-activated depleted fullerene soot for electrochemical double-layer capacitors. Journal of Applied Electrochemistry, 2014, 44, 309-316. 486

#	Article	IF	CITATIONS
487	New synthesis strategies for Ni/Al2O3-Sil-1 core–shell catalysts for steam reforming of methane. Catalysis Today, 2014, 236, 34-40.	2.2	21
488	Towards the Preparation of Ordered Mesoporous Carbon/Carbon Composite Membranes for Gas Separation. Separation Science and Technology, 2014, 49, 171-178.	1.3	21
489	Block copolymer-guided fabrication of shuttle-like polyaniline nanoflowers with radiating whiskers for application in supercapacitors. RSC Advances, 2015, 5, 1016-1023.	1.7	21
490	Utilization of bituminous coal in a direct carbon fuel cell. International Journal of Hydrogen Energy, 2016, 41, 8576-8582.	3.8	21
491	Functional PAN-based monoliths with hierarchical structure for heavy metal removal. Chemical Engineering Journal, 2017, 313, 1607-1614.	6.6	21
492	Microporous MOFs Engaged in the Formation of Nitrogenâ€Doped Mesoporous Carbon Nanosheets for Highâ€Rate Supercapacitors. Chemistry - A European Journal, 2018, 24, 2681-2686.	1.7	21
493	Enhanced electrochemical performances of coal liquefaction residue derived hard carbon coated by graphene as anode materials for sodium-ion batteries. Fuel Processing Technology, 2018, 178, 35-40.	3.7	21
494	In Situ Growing Chromium Oxynitride Nanoparticles on Carbon Nanofibers to Stabilize Lithium Deposition for Lithium Metal Anodes. Small, 2020, 16, e2003827.	5.2	21
495	Dual Hybrid Effect Endowing Nickel–Cobalt Sulfides with Enhanced Cycling Stability for Asymmetrical Supercapacitors. ACS Applied Energy Materials, 2020, 3, 6977-6984.	2.5	21
496	Time-dependent density functional theory study on the coexistent intermolecular hydrogen-bonding and dihydrogen-bonding of the phenol-H2O-diethylmethylsilane complex in electronic excited states. Physical Chemistry Chemical Physics, 2010, 12, 9445.	1.3	20
497	New membrane architecture: ZnO@ZIF-8 mixed matrix membrane exhibiting superb H 2 permselectivity and excellent stability. Inorganic Chemistry Communication, 2014, 48, 77-80.	1.8	20
498	A General, Green Chemistry Approach for Immobilization of Inorganic Catalysts in Monolithic Porous Flow-Reactors. ACS Sustainable Chemistry and Engineering, 2016, 4, 1602-1610.	3.2	20
499	Bis-cyclometalated Ir(III) complexes with a diphenylamino group: design, synthesis, and application in oxygen sensing. Dyes and Pigments, 2017, 136, 641-647.	2.0	20
500	Graphite-graphene architecture stabilizing ultrafine Co3O4 nanoparticles for superior oxygen evolution. Carbon, 2018, 140, 17-23.	5.4	20
501	Ultrafast Construction of Oxygen-Containing Scaffold over Graphite for Trapping Ni ²⁺ into Single Atom Catalysts. ACS Nano, 2020, 14, 11662-11669.	7.3	20
502	Mechanism of coal gasification in a steam medium under arc plasma conditions. Plasma Sources Science and Technology, 2004, 13, 446-453.	1.3	19
503	Controllable preparation of triple-walled carbon nanotubes and their growth mechanism. Chemical Communications, 2007, , 1092.	2.2	19
504	Production of nanosized graphite powders from natural graphite by detonation. Carbon, 2008, 46, 476-481.	5.4	19

#	Article	IF	CITATIONS
505	Preparation of C/CMS composite membranes derived from Poly(furfuryl alcohol) polymerized by iodine catalyst. Desalination, 2009, 249, 486-489.	4.0	19
506	Tailoring of three-dimensional carbon nanotube architectures by coupling capillarity-induced assembly with multiple CVD growth. Journal of Materials Chemistry, 2011, 21, 5967.	6.7	19
507	NH ₄ V ₄ O ₁₀ /rGO Composite as a high-performance electrode material for hybrid capacitive deionization. Environmental Science: Water Research and Technology, 2020, 6, 303-311.	1.2	19
508	Gravity field-mediated synthesis of carbon-conjugated quantum dots with tunable defective density for enhanced triiodide reduction. Nano Energy, 2020, 69, 104377.	8.2	19
509	Synergizing Layered Carbon and Gel Electrolyte for Efficient Energy Storage. ACS Sustainable Chemistry and Engineering, 2020, 8, 4207-4215.	3.2	19
510	Achieving efficient electroreduction CO2 to CO in a wide potential range over pitch-derived ordered mesoporous carbon with engineered Ni-N sites. Journal of CO2 Utilization, 2020, 38, 212-219.	3.3	19
511	Electrolyte/Structure-Dependent Cocktail Mediation Enabling High-Rate/Low-Plateau Metal Sulfide Anodes for Sodium Storage. Nano-Micro Letters, 2021, 13, 178.	14.4	19
512	A tuned Lewis acidic catalyst guided by hard–soft acid–base theory to promote N ₂ electroreduction. Journal of Materials Chemistry A, 2021, 9, 13036-13043.	5.2	19
513	Insight into the Effects of Current Collectors and In Situ Ni Leaching in Highâ€Voltage Aqueous Supercapacitors. Advanced Functional Materials, 2022, 32, .	7.8	19
514	Synthesis of N/P co-doped monolithic hierarchical porous carbon for zinc-ion hybrid capacitors with boosted energy density in ZnSO4/ZnI2 redox electrolyte. Journal of Power Sources, 2022, 542, 231743.	4.0	19
515	Hierarchical Carbonâ€Encapsulated Iron Nanoparticles as a Magnetically Separable Adsorbent for Removing Thiophene in Liquid Fuel. Particle and Particle Systems Characterization, 2013, 30, 637-644.	1.2	18
516	Role of the Electronically Excited-State Hydrogen Bonding and Water Clusters in the Luminescent Metal–Organic Framework. Inorganic Chemistry, 2013, 52, 5742-5748.	1.9	18
517	Efficient synthesis of graphene/sulfur nanocomposites with high sulfur content and their application as cathodes for Li–S batteries. Journal of Materials Chemistry A, 2016, 4, 16219-16224.	5.2	18
518	Layer-dependent catalysis of MoS ₂ /graphene nanoribbon composites for efficient hydrodesulfurization. Catalysis Science and Technology, 2017, 7, 693-702.	2.1	18
519	Nitrogen-doped porous carbon with well-balanced charge conduction and electrocatalytic activity for dye-sensitized solar cells. Carbon, 2018, 128, 201-204.	5.4	18
520	Tailoring the structure and property of microfiltration carbon membranes by polyacrylonitrile-based microspheres for oil-water emulsion separation. Journal of Water Process Engineering, 2019, 32, 100973.	2.6	18
521	Design Principles for Covalent Organic Frameworks to Achieve Strong Heteroatom-Synergistic Effect on Anchoring Polysulfides for Lithium–Sulfur Batteries. Journal of Physical Chemistry Letters, 2019, 10, 7445-7451.	2.1	18
522	A Phase Transformationâ€Resistant Electrode Enabled by a MnO ₂ â€Confined Effect for Enhanced Energy Storage. Advanced Functional Materials, 2019, 29, 1901342.	7.8	18

#	Article	IF	CITATIONS
523	Solar-driven simultaneous desalination and power generation enabled by graphene oxide nanoribbon papers. Journal of Materials Chemistry A, 2022, 10, 9184-9194.	5.2	17
524	Rational-design heteroatom-doped cathode and ion modulation layer modified Zn anode for ultrafast zinc-ion hybrid capacitors with simultaneous high power and energy densities. Journal of Power Sources, 2022, 536, 231484.	4.0	17
525	Sulfur & nitrogen co-doped electrospun carbon nanofibers as freestanding electrodes for membrane capacitive deionization. Separation and Purification Technology, 2022, 295, 121280.	3.9	17
526	Multi-walled carbon nanotubes supported Pt-Fe cathodic catalyst for direct methanol fuel cell. Reaction Kinetics and Catalysis Letters, 2004, 82, 235-240.	0.6	16
527	Development of surface porosity and catalytic activity in metal sludge/waste oil derived adsorbents: Effect of heat treatment. Chemical Engineering Journal, 2008, 138, 155-165.	6.6	16
528	Preparation and mechanical properties of highly-aligned carbon micro-trees. Carbon, 2010, 48, 1926-1931.	5.4	16
529	2â€Phenylquinolineâ€Based Cyclometalated Platinum(II) Complexes: Synthesis and Structure–Photoelectric Properties Relationship in Oxygen Sensing. ChemPlusChem, 2014, 79, 1472-1481.	1.3	16
530	Recyclable catalyst for catalytic hydrogenation of phenylacetylene by coupling Pd nanoparticles with highly compressible graphene aerogels. RSC Advances, 2014, 4, 59977-59980.	1.7	16
531	Copper-catalyzed protodeboronation of arylboronic acids in aqueous media. RSC Advances, 2014, 4, 54307-54311.	1.7	16
532	Colloidally Stabilized Magnetic Carbon Nanotubes Providing MRI Contrast in Mouse Liver Tumors. Biomacromolecules, 2015, 16, 790-797.	2.6	16
533	Chemically converting graphene oxide to graphene with organic base for Suzuki reaction. Materials Research Bulletin, 2015, 67, 77-82.	2.7	16
534	Preparation and characterization of electrospun poly(phthalazinone ether nitrile ketone) membrane with novel thermally stable properties. Applied Surface Science, 2015, 351, 169-174.	3.1	16
535	An electrocatalyst with anti-oxidized capability for overall water splitting. Nano Research, 2018, 11, 3411-3418.	5.8	16
536	Insight into the impact of surface hydrothermal carbon layer on photocatalytic performance of ZnO nanowire. Applied Catalysis A: General, 2019, 583, 117145.	2.2	16
537	Integration of Desulfurization and Lithium–Sulfur Batteries Enabled by Aminoâ€Functionalized Porous Carbon Nanofibers. Energy and Environmental Materials, 2023, 6, .	7.3	16
538	Nitrogen-doped hollow carbon nanoboxes in zwitterionic polymer hydrogel electrolyte for superior quasi-solid-state zinc-ion hybrid supercapacitors. Journal of Materials Chemistry A, 2022, 10, 12856-12868.	5.2	16
539	Novel fluffy carbon balls obtained from coal which consist of short curly carbon fibres. Carbon, 2004, 42, 2359-2362.	5.4	15
540	Adsorption of Aromatic Heterocyclic Compounds on Pristine and Defect Graphene: A First-Principles Study. Journal of Computational and Theoretical Nanoscience, 2011, 8, 2492-2497.	0.4	15

#	Article	IF	CITATIONS
541	Magnetically recyclable Pt/C(Ni) nanocatalysts with improved selectivity for hydrogenation of o-chloronitrobenzene. Catalysis Communications, 2012, 28, 69-72.	1.6	15
542	Preparation and characterization of supported ordered nanoporous carbon membranes for gas separation. Journal of Applied Polymer Science, 2014, 131, .	1.3	15
543	Easy synthesis of MnO-graphene hybrids for high-performance lithium storage. New Carbon Materials, 2014, 29, 316-321.	2.9	15
544	Fabrication and Application of Catalytic Carbon Membranes for Hydrogen Production from Methanol Steam Reforming. Industrial & Engineering Chemistry Research, 2015, 54, 623-632.	1.8	15
545	Quaternary Ammonium Compound Functionalized Activated Carbon Electrode for Capacitive Deionization Disinfection. ACS Sustainable Chemistry and Engineering, 2018, 6, 17204-17210.	3.2	15
546	Hydrogenâ€Bonding Triggered Assembly to Configure Hollow Carbon Nanosheets for Highly Efficient Triâ€lodide Reduction. Advanced Functional Materials, 2020, 30, 2006270.	7.8	15
547	Pd–silicalite-1 composite membrane reactor for direct hydroxylation of benzene to phenol. Catalysis Today, 2010, 156, 282-287.	2.2	14
548	Carbon dioxide-assisted fabrication of self-organized tubular carbon micropatterns on silicon substrates. Carbon, 2010, 48, 1465-1472.	5.4	14
549	Electrically driven light emission from a single suspended carbon nanocoil. Carbon, 2012, 50, 5537-5542.	5.4	14
550	Activated nitrogen-doped carbons from polyvinyl chloride for high-performance electrochemical capacitors. Journal of Solid State Electrochemistry, 2014, 18, 49-58.	1.2	14
551	Palladium-catalyzed ligand-free and efficient Suzuki–Miyaura reaction of heteroaryl halides with MIDA boronates in water. RSC Advances, 2015, 5, 54312-54315.	1.7	14
552	A strategy for regulating the performance of DCFC with semi-coke fuel. International Journal of Hydrogen Energy, 2018, 43, 7465-7472.	3.8	14
553	Co ion-intercalation amorphous and ultrathin microstructure for high-rate oxygen evolution. Energy Storage Materials, 2018, 10, 291-296.	9.5	14
554	A wearable strain sensor based on carbon derived from linen fabrics. New Carbon Materials, 2020, 35, 522-530.	2.9	14
555	Decoupling the role of carbon counterparts in Pickering emulsifier for an enhanced selective oxidation of benzyl alcohol. Green Chemistry, 2020, 22, 5711-5721.	4.6	14
556	Balanced kinetics between electrodes by carbon cloth@ZIF-8 for high rate performance zinc-ion hybrid capacitors. Chemical Communications, 2021, 57, 8778-8781.	2.2	14
557	Mechanochemical coordination self-assembly for Cobalt-based metal-organic framework-derived bifunctional oxygen electrocatalysts. Journal of Colloid and Interface Science, 2022, 613, 733-746.	5.0	14
558	Synthesis and Raman scattering study of double-walled carbon nanotube peapods. Solid State Communications, 2006, 137, 654-657.	0.9	13

#	Article	IF	CITATIONS
559	Role of oil derived carbonaceous phase in the performance of sewage sludge-based materials as media for desulfurizaton of digester gas. Applied Surface Science, 2008, 254, 2385-2395.	3.1	13
560	Effect of microwave-treatment time on the properties of activated carbons for electrochemical capacitors. New Carbon Materials, 2011, 26, 313-319.	2.9	13
561	Preparation of ZIF-8 membranes supported on macroporous carbon tubes via a dipcoating–rubbing method. Journal of Physics and Chemistry of Solids, 2015, 77, 23-29.	1.9	13
562	One-pot to fabrication of calcium oxide/carbon foam composites for the adsorption of trace SO2. Chemical Engineering Journal, 2015, 259, 894-899.	6.6	13
563	Bio-inspired immobilization of metal oxides on monolithic microreactor for continuous Knoevenagel reaction. Journal of Colloid and Interface Science, 2016, 481, 100-106.	5.0	13
564	Synthesis of 3D Flowerâ€like Nanocomposites of Nitrogenâ€Doped Carbon Nanosheets Embedded with Hollow Cobalt(II,III) Oxide Nanospheres for Lithium Storage. ChemElectroChem, 2017, 4, 102-108.	1.7	13
565	DBD plasma-tuned functionalization of edge-enriched graphene nanoribbons for high performance supercapacitors. Electrochimica Acta, 2020, 337, 135741.	2.6	13
566	Activity descriptor of Ni,N-Codoped carbon electrocatalyst in CO2 electroreduction reaction. Chemical Engineering Journal, 2022, 433, 131965.	6.6	13
567	Engineering local environment of ruthenium by defect-tuned SnO2 over carbon cloth for neutral-media N2 electroreduction. Carbon, 2022, 195, 199-206.	5.4	13
568	Recent advances in the electroreduction of carbon dioxide to formic acid over carbon-based materials. New Carbon Materials, 2022, 37, 277-287.	2.9	13
569	Ultra-selective microfiltration SiO2/carbon membranes for emulsified oil-water separation. Journal of Environmental Chemical Engineering, 2022, 10, 107848.	3.3	13
570	Filling double-walled carbon nanotubes with AgCl nanowires. Scripta Materialia, 2008, 58, 457-460.	2.6	12
571	Timeâ€dependent density functional theory study on excitedâ€state dihydrogen bonding OH··ĤGe of the dihydrogenâ€bonded phenolâ€triethylgermanium complex. Journal of Computational Chemistry, 2010, 31, 2853-2858.	1.5	12
572	Role of the intermolecular and intramolecular hydrogen bonding on the excited-state proton transfer behavior of 3-aminophthalimide (3AP) dimer. Journal of Photochemistry and Photobiology A: Chemistry, 2011, 217, 219-223.	2.0	12
573	SiO <i>_x</i> Nanowire Assemblies Grown by Floating Catalyst Method. Materials Express, 2012, 2, 157-163.	0.2	12
574	Preparing electrochemical active hierarchically porous carbons for detecting nitrite in drinkable water. RSC Advances, 2016, 6, 7302-7309.	1.7	12
575	From diverse polycyclic aromatic molecules to interconnected graphene nanocapsules for supercapacitors. Microporous and Mesoporous Materials, 2017, 245, 73-81.	2.2	12
576	Graphene oxide induced fabrication of pillared and double-faced polyaniline arrays with enhanced triiodide reduction capability. Electrochimica Acta, 2017, 252, 84-90.	2.6	12

#	Article	IF	CITATIONS
577	Sulfidation of iron confined in nitrogen-doped carbon nanotubes to prepare novel anode materials for lithium ion batteries. New Carbon Materials, 2018, 33, 544-553.	2.9	12
578	Investigation of the attapulgite hybrid carbon molecular sieving membranes for permanent gas separation. Chemical Engineering Research and Design, 2019, 151, 146-156.	2.7	12
579	Hierarchical Bimetallic Hydroxides Built by Porous Nanowire‣apped Bundles with Ultrahigh Areal Capacity for Stable Hybrid Solid‣tate Supercapacitors. Advanced Materials Interfaces, 2019, 6, 1900959.	1.9	12
580	The positive/negative effects of bentonite on O2/N2 permeation of carbon molecular sieving membranes. Microporous and Mesoporous Materials, 2019, 285, 142-149.	2.2	12
581	Ion removal performance and enhanced cyclic stability of SnO2/CNT composite electrode in hybrid capacitive deionization. Materials Today Communications, 2020, 23, 100904.	0.9	12
582	Fabrication of nitrogen-doped porous graphene hybrid nanosheets from metal–organic frameworks for lithium-ion batteries. Nanotechnology, 2020, 31, 145402.	1.3	12
583	Fabrication of Porous Carbon Nanosheets with the Engineered Graphitic Structure for Electrochemical Supercapacitors. Industrial & Engineering Chemistry Research, 2020, 59, 13623-13630.	1.8	12
584	Recent Advances in the Synthesis and Applications of Carbon Dots. Wuli Huaxue Xuebao/ Acta Physico - Chimica Sinica, 2019, 35, 572-590.	2.2	12
585	The formation mechanism of CO2and its conversion in the process of coal gasification under arc plasma conditions. Plasma Sources Science and Technology, 2006, 15, 246-252.	1.3	11
586	Controlled preparation of unsupported binary and ternary sulfides with high surface area from tetraalkylammonium thiosalts. Journal of Physics and Chemistry of Solids, 2010, 71, 642-646.	1.9	11
587	The effect of furcated hydrogen bond and coordination bond on luminescent behavior of metal-organic framework [CuCN·EIN]: A TDDFT study. Spectrochimica Acta - Part A: Molecular and Biomolecular Spectroscopy, 2012, 97, 589-593.	2.0	11
588	Time-dependent density functional theory study on the electronic excited-state hydrogen bonding of the chromophore coumarin 153 in a room-temperature ionic liquid. Journal of Molecular Modeling, 2012, 18, 937-945.	0.8	11
589	Oxygenâ€promoted Palladiumâ€onâ€Carbonâ€catalyzed Ligandâ€free Suzuki Reaction for the Synthesis of Heterobiaryls in Aqueous Media. Asian Journal of Organic Chemistry, 2013, 2, 514-518.	1.3	11
590	A facile soft-template synthesis of nitrogen dopedÂmesoporous carbons for hydrogen sulfide removal. Adsorption, 2016, 22, 1075-1082.	1.4	11
591	Synthesis of highly oriented stacked tile-like carbon sheet for potassium storage. Materials Letters, 2020, 277, 128134.	1.3	11
592	Achieving Multiple and Tunable Ratios of Syngas to Meet Various Downstream Industrial Processes. ACS Sustainable Chemistry and Engineering, 2020, 8, 3328-3335.	3.2	11
593	Fabrication, magnetic properties and self-assembly of hierarchical crystalline hexapod magnetites. RSC Advances, 2012, 2, 4329.	1.7	10
594	Substituent effects on the photophysical and electrochemical properties of iridium(III) complexes containing an arylcarbazolyl moiety. Dyes and Pigments, 2014, 109, 13-20.	2.0	10

#	Article	IF	CITATIONS
595	Preparation of Single-Walled Carbon Nanotubes from Fullerene Waste Soot. ACS Sustainable Chemistry and Engineering, 2014, 2, 14-18.	3.2	10
596	Folding of graphene into elastic nanobelts. Carbon, 2014, 76, 46-53.	5.4	10
597	Theoretical and Experimental Insights into the Effects of Oxygen-Containing Species within CNTs toward Triiodide Reduction. ACS Sustainable Chemistry and Engineering, 2019, 7, 7527-7534.	3.2	10
598	Mechanochemistry-driven prelinking enables ultrahigh nitrogen-doping in carbon materials for triiodide reduction. Nano Energy, 2021, 89, 106332.	8.2	10
599	Pickering Emulsion Catalysis: Interfacial Chemistry, Catalyst Design, Challenges, and Perspectives. Angewandte Chemie, 2022, 134, .	1.6	10
600	Self-assembly of carbon nanotube polyhedrons inside microchannels. Chemical Communications, 2008, , 2747.	2.2	9
601	Time-dependent density functional theory study on electronic excited states of the hydrogen-bonded solute–solvent phenol–(H2O)n (n=3–5) clusters. Journal of Luminescence, 2011, 131, 2279-2285.	1.5	9
602	Hydrogen bonding and coordination bonding in the electronically excited states of the MOF Cu2 (L)2 (L=5-(4-pyridyl)tetrazole) CH2Cl2: A time-dependent density functional theory study. Journal of Luminescence, 2013, 142, 110-115.	1.5	9
603	Molecular simulation of adsorption of NO and CO2 mixtures by a Cu-BTC metal organic framework. Current Applied Physics, 2015, 15, 1070-1074.	1.1	9
604	Theoretical design and experimental synthesis of counter electrode for dye-sensitized solar cells: Amino-functionalized graphene. Journal of Energy Chemistry, 2016, 25, 861-867.	7.1	9
605	Preparing a highly dispersed catalyst supported on mesoporous microspheres via the self-assembly of amphiphilic ligands for the recovery of ultrahigh concentration wastewater. Journal of Materials Chemistry A, 2016, 4, 6304-6312.	5.2	9
606	Energy Accumulation Enabling Fast Synthesis of Intercalated Graphite and Operando Decoupling for Lithium Storage. Advanced Functional Materials, 2021, 31, 2009801.	7.8	9
607	Preparation of Nanoscale CexFe1-xO2 Solid Solution Catalyst by the Template Method and Its Catalytic Properties for Ethanol Steam Reforming. Chinese Journal of Catalysis, 2008, 29, 418-420.	6.9	8
608	A facile approach to simultaneous fabrication of microsize hollow and solid carbon spheres from acetylene directly. Materials Letters, 2008, 62, 581-583.	1.3	8
609	Efficient synthesis of 4â€heteroarylâ€substituted triphenylamine derivatives via a ligandâ€free Suzuki reaction. Applied Organometallic Chemistry, 2011, 25, 862-866.	1.7	8
610	A theoretical forecast of the hydrogen bond changes in the electronic excited state for BN and its derivatives. Open Physics, 2012, 10, .	0.8	8
611	Releasing 9.6Âwt% of H2 from Mg(NH2)2–3LiH–NH3BH3 through mechanochemical reaction. International Journal of Hydrogen Energy, 2013, 38, 10446-10452.	3.8	8
612	Structure and gas permeation of nanoporous carbon membranes based on RF resin/F-127 with variable catalysts. Journal of Materials Research, 2014, 29, 2881-2890.	1.2	8

#	Article	IF	CITATIONS
613	Controlled Fabrication of Interconnected Porous Carbon Nanosheets for Supercapacitors with a Long Cycle Life. ChemElectroChem, 2017, 4, 3196-3203.	1.7	8
614	Enhanced separation performance of microfiltration carbon membranes for oily wastewater treatment by an air oxidation strategy. Chemical Engineering and Processing: Process Intensification, 2021, 169, 108620.	1.8	8
615	A Lowâ€Temperature Dehydration Carbonâ€Fixation Strategy for Lignocelluloseâ€Based Hierarchical Porous Carbon for Supercapacitors. ChemSusChem, 2022, 15, .	3.6	8
616	Electric-Field-Triggered Graphene Production: From Fundamental Energy Applications to Perspectives. Accounts of Materials Research, 2022, 3, 175-186.	5.9	8
617	Interlayerâ€Expanded Titanate Hierarchical Hollow Spheres Embedded in Carbon Nanofibers for Enhanced Na Storage. Small, 2022, 18, e2107890.	5.2	8
618	States of Carbon Nanotube Supported Mo-Based HDS Catalysts. Journal of Natural Gas Chemistry, 2006, 15, 203-210.	1.8	7
619	Microporous carbon membranes from sulfonated poly(phthalazinone ether sulfone ketone): Preparation, characterization, and gas permeation. Journal of Applied Polymer Science, 2011, 122, 1190-1197.	1.3	7
620	Improvements of heat resistance and adhesive property of condensed poly-nuclear aromatic resin via epoxy resin modification. Petroleum Science, 2014, 11, 578-583.	2.4	7
621	Surface Modification of Multiwalled Carbon Nanotubes with Engineered Self-Assembled RAFT Diblock Coatings. Australian Journal of Chemistry, 2014, 67, 151.	0.5	7
622	Cyclometalated Ir(III) complexes-catalyzed aerobic hydroxylation of arylboronic acids induced by visible-light. Tetrahedron, 2017, 73, 3031-3035.	1.0	7
623	Effect of a heat pretreatment on the structure and properties of carbon supports for carbon membranes. Canadian Journal of Chemical Engineering, 2017, 95, 2112-2119.	0.9	7
624	Template-free synthesis of interconnected carbon nanosheets <i>via</i> cross-linking coupled with annealing for high-efficiency triiodide reduction. Green Chemistry, 2018, 20, 250-254.	4.6	7
625	A Câ€Sâ€C Linkageâ€Triggered Ultrahigh Nitrogenâ€Doped Carbon and the Identification of Active Site in Triiodide Reduction. Angewandte Chemie, 2021, 133, 3631-3639.	1.6	7
626	Time-dependent density functional theory study of the excited-state dihydrogen bonding: clusters of 2-pyridone with diethylmethylsilane and triethylgermanium. Journal of Molecular Modeling, 2011, 17, 1891-1897.	0.8	6
627	Synthesis and characterization of condensed poly-nuclear aromatic resin using heavy distillate from ethylene tar. New Carbon Materials, 2012, 27, 469-475.	2.9	6
628	Calixarene building block bis(2-hydroxyphenyl)methane (2HDPM) and hydrogen-bonded 2HDPM-H2O complex in electronic excited state. Journal of Molecular Modeling, 2013, 19, 1913-1918.	0.8	6
629	Interconnected polyaniline clusters constructed from nanowires: Confined polymerization and electrochemical properties. Journal of Materials Research, 2014, 29, 2408-2415.	1.2	6
630	Elucidating photodehalogenation mechanisms of polychlorinated and polybrominated dibenzo-p-dioxins and dibenzofurans and Mg2+ effects by quantum chemical calculations. Computational and Theoretical Chemistry, 2014, 1042, 49-56.	1.1	6

#	Article	IF	CITATIONS
631	Synthesis of low Si/Al ratio hydroxysodalite from oil shale ash without pretreatment. Journal of Chemical Technology and Biotechnology, 2015, 90, 208-212.	1.6	6
632	Process Intensification of the Hydrogen Production Reaction Using a Carbon Membrane Reactor: Kinetics Analysis. Energy Technology, 2017, 5, 1990-1997.	1.8	6
633	Multilevel Coupled Hybrids Made of Porous Cobalt Oxides and Graphene for Highâ€Performance Lithium Storage. Chemistry - A European Journal, 2019, 25, 5527-5533.	1.7	6
634	Monolithic carbon nanosheets with rich pores for high-capacitance supercapacitor. Journal of Porous Materials, 2020, 27, 487-494.	1.3	6
635	Interface Inversion: A Promising Strategy to Configure Ultrafine Nanoparticles over Graphene for Fast Sodium Storage. Small, 2021, 17, 2005119.	5.2	6
636	A nickel-nitrogen-doped carbon foam as monolithic electrode for highly efficient CO2 electroreduction. Journal of CO2 Utilization, 2021, 49, 101549.	3.3	6
637	Highly permeable and selective sepiolite hybrid mixed matrix carbon membranes supported on plate carbon substrates for gas separation. Chemical Engineering Research and Design, 2021, 174, 319-330.	2.7	6
638	Insight into the Inhibition of Shuttle by Metal-Modified Covalent Triazine Frameworks and Graphene Composites with the Solvent Interaction in Lithium Sulfur Batteries. ACS Applied Energy Materials, 2022, 5, 825-831.	2.5	6
639	Multilayer-Dense Porous Carbon Nanosheets with High Volumetric Capacitance for Supercapacitors. Industrial & Engineering Chemistry Research, 2022, 61, 8908-8917.	1.8	6
640	Synthesis and Characterization of Carbon-Encapsulated Magnetic Nanoparticles via Arc-Plasma Assisted CVD. Journal of Nanoscience and Nanotechnology, 2009, 9, 7473-6.	0.9	5
641	Flower-Like Co-Ni/C Bimetallic Catalysts for the Selective Hydrogenation of o-Chloronitrobenzene. Chinese Journal of Catalysis, 2012, 33, 1883-1888.	6.9	5
642	Theoretical Study of Oxygen Chemisorption on Pd (111), Au (111) and Pd–Au (111) Alloy Surfaces. Journal of Computational and Theoretical Nanoscience, 2012, 9, 394-400.	0.4	5
643	Theoretical studies on how excited state hydrogen and coordination bonds affect luminescent properties of Metal Organic Framework Cu4(L)4•2EtOH. Inorganic Chemistry Communication, 2013, 31, 69-73.	1.8	5
644	Palladium-catalyzed ligand-free and efficient SuzukiMiyaura reaction of \$N\$-methyliminodiacetic acid boronates in water. Turkish Journal of Chemistry, 2015, 39, 1208-1215.	0.5	5
645	Ni Modified WCx Catalysts for Methane Dry Reforming. ACS Symposium Series, 2015, , 171-189.	0.5	5
646	Why Wasn't My <i>ACS Sustainable Chemistry & Engineering</i> Manuscript Sent Out for Review?. ACS Sustainable Chemistry and Engineering, 2019, 7, 1-2.	3.2	5
647	Silicaâ€Assisted Fabrication of Nâ€doped Porous Carbon for Efficient Electrocatalytic Nitrogen Fixation. ChemCatChem, 2020, 12, 3453-3458.	1.8	5
648	Recent advances in multilevel nickel-nitrogen-carbon catalysts for CO2electroreduction to CO. New Carbon Materials, 2021, 36, 19-33.	2.9	5

#	Article	IF	CITATIONS
649	Highly efficient & economic synthesis of CoS1.097/nitrogen-doped carbon for enhanced triiodide reduction. Carbon, 2021, 174, 445-450.	5.4	5
650	Hydrogen Production and Water Desalination with Onâ€demand Electricity Output Enabled by Electrochemical Neutralization Chemistry. Angewandte Chemie, 2022, 134, .	1.6	5
651	Molecular dynamics study of hydrogen adsorption in Y-junction carbon nanotubes. Computational and Theoretical Chemistry, 2004, 684, 75-80.	1.5	4
652	Synthesis of Cs-filled double-walled carbon nanotubes by a plasma process. Carbon, 2006, 44, 1586-1589.	5.4	4
653	Time-Dependent Density Functional Theory Study on Hydrogen and Dihydrogen Bonding in Electronically Excited State of 2-Pyridone–Borane–Trimethylamine Cluster. Journal of Cluster Science, 2013, 24, 459-470.	1.7	4
654	Synthesis and structure of carbon belts made of carbon nanofibers supported on carbon foams. Carbon, 2013, 61, 386-394.	5.4	4
655	Synthesis of boron, nitrogen co-doped porous carbon from asphaltene for high-performance supercapacitors. Chinese Physics B, 2014, 23, 086101.	0.7	4
656	Preparation of graphene from Taixi anthracite and its photocatalyst performance for CO ₂ conversion. Proceedings of the Institution of Mechanical Engineers, Part N: Journal of Nanoengineering and Nanosystems, 2014, 228, 61-64.	0.1	4
657	Effect of CH3OH on the luminescent properties of the [Zn(sfdb)(bpy)(H2O)] · 0.5nCH3OH metal–organic framework. Chemical Physics, 2015, 446, 65-69.	0.9	4
658	CoMn Layered Double Hydroxides/Carbon Nanotubes Architectures as High-Performance Electrocatalysts for the Oxygen Evolution Reaction. ChemElectroChem, 2016, 3, 850-850.	1.7	4
659	Salinityâ€Differenceâ€Driven Power Generation by a Hybrid Capacitive Approach. Energy Technology, 2018, 6, 238-241.	1.8	4
660	Passivating the pHâ€Responsive Sites to Configure a Widely pHâ€Stable Emulsifier for Highâ€Efficiency Benzyl Alcohol Oxidation. ChemSusChem, 2022, 15, .	3.6	4
661	The interaction between C28 (Td) and X (X=H and F). Computational and Theoretical Chemistry, 2006, 760, 53-57.	1.5	3
662	Pore structure prediction of coal-based microfiltration carbon membranes. Science Bulletin, 2010, 55, 1325-1330.	1.7	3
663	Time-dependent density functional theory study on the hydrogen bonding in electronic excited states of 6-amino-3-((thiophen-2-yl) methylene)-phthalide in methanol solution. Computational and Theoretical Chemistry, 2011, 972, 57-62.	1.1	3
664	The Interaction Between an Oxygen Atom and C ₇₀ (<i>D</i> _{5<i>h</i>}): A Density Functional Theory Study. Journal of Computational and Theoretical Nanoscience, 2011, 8, 2429-2433.	0.4	3
665	Formation mechanism of hollow silicon ingot induced by fountain effect. Renewable Energy, 2015, 77, 463-466.	4.3	3
666	A Dual Component Catalytic System Composed of Nonâ€Noble Metal Oxides for Li–O ₂ Batteries with Enhanced Cyclability. Particle and Particle Systems Characterization, 2016, 33, 228-234.	1.2	3

#	Article	IF	CITATIONS
667	Coaxial heterojunction carbon nanofibers with charge transport and electrocatalytic reduction phases for high performance dye-sensitized solar cells. RSC Advances, 2018, 8, 7040-7043.	1.7	3
668	Effects of Diatomaceous Earth Addition on the Microstructure and Gas Permeation of Carbon Molecular Sieving Membranes. ChemistrySelect, 2018, 3, 8428-8435.	0.7	3
669	Lowâ€Temperature Fast Production of Carbon and Acetic Acid Dualâ€Promoted Pd/C Catalysts. Chemistry - A European Journal, 2019, 25, 13683-13687.	1.7	3
670	Physical Design, Preparation and Functionalization of Carbon Membranes for Gas Separation. Wuji Cailiao Xuebao/Journal of Inorganic Materials, 2010, 25, 449-456.	0.6	3
671	Hydrogen Bonding Dynamics of Phenol-(H ₂ O) ₂ Cluster in the Electronic Excited State: a DFT/TDDFT Study. Journal of the Korean Chemical Society, 2011, 55, 385-391.	0.2	3
672	Fabrication of 3D Co3O4 Homoarchitectures via a Novel Template-assisted Coprecipitation Process. Chemistry Letters, 2010, 39, 944-945.	0.7	2
673	ELECTRON TRANSFER MAKES D3h (78:5) CAGE EASY TO FORM M2@C78(M = La, Ce): A RELATIVISTIC DENSITY-FUNCTIONAL THEORY STUDY. Journal of Theoretical and Computational Chemistry, 2012, 11, 197-207.	1.8	2
674	The Hydrogen Bonding in Electronically Excited States of the Luminescent Metal-Organic Frameworks Containing H2O: Time-Dependent Density Functional Theory Study. Journal of Computational and Theoretical Nanoscience, 2013, 10, 2088-2093.	0.4	2
675	Monolithic Electrodes: Ultrafast Selfâ€Assembly of Graphene Oxideâ€Induced Monolithic NiCo–Carbonate Hydroxide Nanowire Architectures with a Superior Volumetric Capacitance for Supercapacitors (Adv. Funct. Mater. 14/2015). Advanced Functional Materials, 2015, 25, 2203-2203.	7.8	2
676	Facile one-step synthesis of highly graphitized hierarchical porous carbon nanosheets with large surface area and high capacity for lithium storage. RSC Advances, 2016, 6, 51146-51152.	1.7	2
677	A simple oneâ€step dropâ€coating approach on fabrication of supported carbon molecular sieve membranes with high gas separation performance. Asia-Pacific Journal of Chemical Engineering, 2018, 13, e2251.	0.8	2
678	Synthesis and Properties of Hierarchical Macro-mesoporous Carbon Materials. Wuji Cailiao Xuebao/Journal of Inorganic Materials, 2011, 26, 145-148.	0.6	2
679	Sidewall fluorination and hydrogenation of single-walled carbon nanotubes: a density functional theory study. Frontiers of Physics in China, 2009, 4, 393-397.	1.0	1
680	The Electronically Excited-State of the MFU-4 [Zn ₅ Cl ₄ (BBTA) ₃] Metal-Organic Frameworks: Time-Dependent Density Functional Theory Study. Journal of Computational and Theoretical Nanoscience, 2013, 10, 1477-1482.	0.4	1
681	Theoretical study of the interaction between X (H, F) and graphene. Molecular Simulation, 2014, 40, 306-312.	0.9	1
682	Structural characterization and properties of ODPA–ODA polyetherimide membranes modified by ethylene glycol. Polymer Bulletin, 2018, 75, 5825-5842.	1.7	1
683	The thickening of carbon fibers via a 3D island growth mechanism: New insights from a theoretical and experimental study. Carbon, 2019, 152, 851-854.	5.4	1
684	Glutamic acid-assisted hydrothermal recrystallization to configure bamboo-like carbon nanotubes for improved triiodide reduction. Chinese Journal of Chemical Engineering, 2021, 37, 159-167.	1.7	1

#	Article	IF	CITATIONS
685	Continuous-flow Synthesis of Submicron and Nano-zeolites in Capillary Micro-channel Reactor. Wuji Cailiao Xuebao/Journal of Inorganic Materials, 2011, 26, 1304-1308.	0.6	1
686	Facile synthesis of mono-, bis- and tris-aryl-substituted aniline derivatives in aqueous DMF. Arkivoc, 2013, 2012, 62-75.	0.3	1
687	S, N co-doped pitch-based composite carbon nanofibers with enlarged interlayer distance as a superior potassium ion batteries anode. E3S Web of Conferences, 2020, 213, 02003.	0.2	1
688	Direct Synthesis of Ultrathin Two-Dimensional Co-Based Metal–Organic Framework Membranes by the Conversion of Co(OH) ₂ Sheets for Gas Separation. Industrial & Engineering Chemistry Research, 2022, 61, 9847-9855.	1.8	1
689	Simulation study of hydrogen storage in two kinds of Y-junction carbon nanotubes. , 0, , .		Ο
690	Modification of Double-Walled Carbon Nanotubes by Cs Plasma Ion Irradiation. Japanese Journal of Applied Physics, 2006, 45, 8330-8334.	0.8	0
691	The Interactions of <i>T_d</i> -C ₄₀ , <i>T_d</i> -C ₅₆ with X (X = H, F) by Density Function Theory. Journal of Computational and Theoretical Nanoscience, 2009, 6, 1591-1595.	0.4	0
692	The Interaction Between C ₃₆ (<i>D</i> _{6<i>h</i>}) and X Atom (X) T	j E đQ qO O	0 o gBT /Ove
693	The interaction between D3h–C74 and fluorine. Computational and Theoretical Chemistry, 2011, 963, 314-318.	1.1	0
694	Plasma-Assisted Chemical Vapor Deposition of Titanium Oxide Films by Dielectric Barrier Discharge in TiCl4/O2/N2Gas Mixtures. Plasma Science and Technology, 2014, 16, 695-700.	0.7	0

695	<i>Operando</i> Leaching of Pre-Incorporated Al and Mechanism in Transition Metal Hybrids for Elaborately Enhanced Charge Storage. SSRN Electronic Journal, 0, , .	0.4	0	
-----	---	-----	---	--